

Circulation

JOURNAL OF THE AMERICAN HEART ASSOCIATION



Survival and Cardiac Remodeling After Myocardial Infarction Are Critically Dependent on the Host Innate Immune Interleukin-1 Receptor-Associated Kinase-4 Signaling: A Regulator of Bone Marrow-Derived Dendritic Cells

Yuichiro Maekawa, Nobuo Mizue, Annie Chan, Yu Shi, Youan Liu, Steven Dawood, Manyin Chen, Fayez Dawood, Geoffrey de Couto, Guo Hua Li, Nobutaka Suzuki, Wen-Chen Yeh, Anthony Gramolini, Jeffrey A. Medin and Peter P. Liu

Circulation 2009;120:1401-1414; originally published online Sep 21, 2009;

DOI: 10.1161/CIRCULATIONAHA.109.865956

Circulation is published by the American Heart Association, 7272 Greenville Avenue, Dallas, TX 72514

Copyright © 2009 American Heart Association. All rights reserved. Print ISSN: 0009-7322. Online ISSN: 1524-4539

The online version of this article, along with updated information and services, is located on the World Wide Web at:

<http://circ.ahajournals.org/cgi/content/full/120/14/1401>

Data Supplement (unedited) at:

<http://circ.ahajournals.org/cgi/content/full/CIRCULATIONAHA.109.865956/DC1>

Subscriptions: Information about subscribing to *Circulation* is online at
<http://circ.ahajournals.org/subscriptions/>

Permissions: Permissions & Rights Desk, Lippincott Williams & Wilkins, a division of Wolters Kluwer Health, 351 West Camden Street, Baltimore, MD 21202-2436. Phone: 410-528-4050. Fax: 410-528-8550. E-mail:
journalpermissions@lww.com

Reprints: Information about reprints can be found online at
<http://www.lww.com/reprints>

Survival and Cardiac Remodeling After Myocardial Infarction Are Critically Dependent on the Host Innate Immune Interleukin-1 Receptor–Associated Kinase-4 Signaling

A Regulator of Bone Marrow–Derived Dendritic Cells

Yuichiro Maekawa, MD, PhD; Nobuo Mizue, MD, PhD; Annie Chan, MSc; Yu Shi, MD, PhD; Youan Liu, MD, MSc; Steven Dawood, BSc; Manyin Chen, MD, MSc; Fayez Dawood, DVM; Geoffrey de Couto, BSc; Guo Hua Li, MD, PhD; Nobutaka Suzuki, PhD; Wen-Chen Yeh, MD, PhD; Anthony Gramolini, PhD; Jeffrey A. Medin, PhD; Peter P. Liu, MD

Background—The innate immune system greatly contributes to the inflammatory process after myocardial infarction (MI). Interleukin-1 receptor–associated kinase-4 (IRAK-4), downstream of Toll/interleukin-1 receptor signaling, has an essential role in regulating the innate immune response. The present study was designed to determine the mechanism by which IRAK-4 is responsible for the cardiac inflammatory process, which consequently affects left ventricular remodeling after MI.

Methods and Results—Experimental MI was created in IRAK-4^{-/-} and wild-type mice by left coronary ligation. Mice with a targeted deletion of IRAK-4 had an improved survival rate at 4 weeks after MI. IRAK-4^{-/-} mice also demonstrated attenuated cardiac dilation and decreased inflammation in the infarcted myocardium, which was associated with less proinflammatory and Th1 cytokine expression mediated by suppression of nuclear factor- κ B and c-Jun N-terminal kinase activation. IRAK-4^{-/-} mice had fewer infiltrations of CD45⁺ leukocytes and CD11c⁺ dendritic cells, inhibition of apoptosis, and reduced fibrosis and nitric oxide production. Cardiac dendritic cells in IRAK-4^{-/-} mice were relatively immature or functionally naïve after MI in that they demonstrated less cytokine and costimulatory molecule gene expression. Furthermore, IRAK-4^{-/-} dendritic cells have less mobilization capacity. Transfer of wild type–derived bone marrow dendritic cells into IRAK-4^{-/-} mice for functional dendritic cell reconstitution negated the survival advantage and reduced the cardiac dilation observed with IRAK-4^{-/-} mice at 28 days after MI.

Conclusions—Deletion of IRAK-4 has favorable effects on survival and left ventricular remodeling after MI through modification of the host inflammatory process by blunting the detrimental bone marrow dendritic cells mobilization after myocardial ischemia. (*Circulation*. 2009;120:1401-1414.)

Key Words: blood cells ■ heart failure ■ immune system ■ inflammation ■ myocardial infarction ■ remodeling

The innate immune system is evolutionarily conserved among all multicellular organisms and is the first line of defense against microorganisms through Toll–interleukin-1 receptor (TIR) signaling. However, this system is also activated after various forms of tissue injury and triggers immune responses in the host.¹ We and others have demonstrated that the innate immune system contributes importantly to the progression of myocarditis and the remodeling process after myocardial infarction (MI).^{2–4}

Clinical Perspective on p 1414

Toll-like receptors (TLRs) are type I transmembrane proteins with an extracellular domain containing a leucine-rich repeat and a cytoplasm domain analogous to those of members of the interleukin (IL)-1 receptor family.⁵ After ligand binding, TLRs and IL-1 receptors dimerize and undergo a conformational change required for the recruitment of common downstream signaling molecules. These include the

Received January 19, 2008; accepted July 21, 2009.

From Toronto General Hospital, University Health Network (Y.M., A.C., Y.S., Y.L., S.D., M.C., F.D., G.d.C., G.H.L., P.P.L.); Ontario Cancer Institute, University Health Network (N.M., N.S., W.-C.Y., J.A.M.); and Banting and Best Department of Medical Research (A.G.) and Institute of Circulatory and Respiratory Health (P.P.L.), Canadian Institutes of Health Research, Toronto, Ontario, Canada. Dr Suzuki is currently at Pharmacology Research Laboratories II, Takeda Pharmaceutical Company Ltd, Tukuba, Japan. Dr Yeh is currently at Amgen San Francisco.

The online-only Data Supplement is available with this article at <http://circ.ahajournals.org/cgi/content/full/CIRCULATIONAHA.109.865956/DC1>.

Correspondence to Peter P. Liu, MD, Scientific Director, Canadian Institutes of Health Research, NCSB11–1266, Toronto General Hospital, University Health Network, 200 Elizabeth St, Toronto, Ontario, M5G 2C4, Canada. E-mail peter.liu@utoronto.ca

© 2009 American Heart Association, Inc.

Circulation is available at <http://circ.ahajournals.org>

DOI: 10.1161/CIRCULATIONAHA.109.865956

adaptor molecule myeloid differentiation primary-response protein 88, IL-1 receptor–associated kinases (IRAKs), and tumor necrosis factor (TNF) receptor–associated factor 6 and ultimately lead to translocation of nuclear factor κ B (NF- κ B) for the production of proinflammatory cytokines. IRAK-4, a member of the IRAK family and a downstream protein of TIR signaling, has been shown to play an essential role in mediating signals initiated by IL-1 receptor and TLR engagement.⁶

Dendritic cells (DCs) are a sparsely distributed, migratory group of bone marrow (BM) –derived leukocytes that are major antigen-presenting cells and key players in regulating the innate immune responses through TIR signaling. They have been found in lymphoid and nonlymphoid organs, including heart, liver, thyroid, pancreas, bladder, kidney, ureter, and skin.^{7,8} DCs and their precursors are considered sentinels of the immune system; they circulate through the blood and nonlymphoid peripheral tissues, where they become resident cells over time.⁹ After pathogen invasion or tissue injury, DC precursors accumulate rapidly in the local infected tissues.¹⁰ Zhang et al¹¹ showed that migrating BM-derived DCs (BMDCs) infiltrate into the injured myocardium and participate in the activation of lymphocytes after MI. A recent study demonstrated that DCs regulate the development of autoimmune heart failure through the recognition of heart-specific peptides.¹² These observations suggest that DCs may play a role in inflammation and consequently in tissue remodeling after MI.

Although *in vivo* experiments have shown a cardioprotective effect by inhibition of the innate immune response after MI,^{4,13} the mechanism remains to be identified. To clarify potential mechanisms, we designed the following experiments to answer these questions: Is deletion of IRAK-4, a downstream molecule of TIR signaling, protective against myocardial ischemia? If so, how does IRAK-4 deficiency lead to a favorable host outcome after MI? In the present study, we used IRAK-4^{-/-} mice combined with adoptive transfer and demonstrated that attenuation of TIR signaling and DC function contributed to protecting the heart against MI.

Methods

A detailed Methods section can be found in the online-only Data Supplement.

Experimental Animals

Generation of IRAK-4^{-/-} mice with a mixed 129/Ola;B6 genetic background has been described previously.¹⁴ After mating, homozygous (-/-) and wild-type (+/+) (WT) mice were identified by polymerase chain reaction analysis of DNA obtained from the tail of each mouse, and male homozygous and WT mice were used in this experiment. All procedures were performed in accordance with the Animal Care Committee of the University Health Network of University of Toronto. All mice were housed under identical conditions and given food and water *ad libitum*.

Adoptive DC Transfer

BMDCs (1×10^6 cells per mouse) from WT or IRAK-4^{-/-} mice were resuspended in 40 μ L PBS and then injected into the border zone of myocardium after MI. We confirmed reconstituted BMDCs, which were labeled with the fluorescent dye 5, 6-carboxyfluorescein diacetate succinimidyl ester (CFSE) (Molecular Probes, Carlsbad, Calif) according to the manufacturer's protocol, in WT or

IRAK-4^{-/-} mice under the fluorescent microscope in combination with α -actinin (Sigma-Aldrich, St Louis, Mo) staining.

Additional Methods

The expanded Methods section in the online-only Data Supplement contains information on the creation of MI; hemodynamic measurements; echocardiographic and morphometric analyses; DC isolation from BM; *in vitro* activation of BMDCs; isolation of DCs from the heart; flow cytometry; Western blotting; immunohistochemistry; analysis of myocardial apoptosis; electrophoretic mobility shift assay; TNF- α , IL-6, and IL-12p70 measurements; and quantification of gene expression by real-time polymerase chain reaction.

Statistical Analyses

All values are presented as mean \pm SEM. Analyses of data recorded at a single time point were performed by 2-tailed unpaired Student *t* tests. IRAK-4 expression over time was compared by use of 1-way ANOVA for repeated measurements with posthoc testing. Comparison of expression levels between IRAK-4^{-/-} and WT mice was performed with 2-way ANOVA with posthoc testing. Percentages of DCs were compared by use of 2-way ANOVA for repeated measurements and posthoc testing. Survival rates were compared by the Kaplan–Meier method and analyzed by the log-rank test. Significance was taken as $P < 0.05$. All statistical analyses were performed with Statview 5.0 software (SAS Institute Inc, Cary, NC) and Microsoft Office Excel (Microsoft, Redmond, Wash).

The authors had full access to and take full responsibility for the integrity of the data. All authors have read and agree to the manuscript as written.

Results

Expression of IRAK-4 in the Infarcted Myocardium

We analyzed the IRAK-4 protein level in the infarcted myocardium by immunoblotting. IRAK-4 expression in WT mice was upregulated within 7 days after MI, suggesting that it is a stress-induced protein involved in myocardial inflammation (Figure 1A and 1B).

Improved Survival and Cardiac Function in IRAK-4^{-/-} Mice After MI

All sham-operated mice survived throughout the study. Survival was significantly higher in IRAK-4^{-/-} (76%) compared with WT (36%) mice on day 28 after MI (Figure 1C). Echocardiographic analysis revealed decreased cardiac dilatation and better systolic function in IRAK-4^{-/-} compared with WT infarcted hearts at 28 days. Hemodynamic data also showed that left ventricular (LV) end-systolic pressure and dP/dtmax were significantly greater in IRAK-4^{-/-} than WT mice after MI (the Table). Although there was no significant difference in the ratio of lung weight to body weight between WT and IRAK-4^{-/-} mice, the ratio of heart weight to body weight in IRAK-4^{-/-} mice was significantly lower than in WT mice after MI (the Table).

Comparisons of Infarct Sizes Between WT and IRAK-4^{-/-} Mice

Although the size of the MI on day 3 was similar between WT and IRAK-4^{-/-} mice, the infarct in the mice at 28 days after MI tended to be smaller in IRAK-4^{-/-} than WT mice (Figure 1D and 1E).

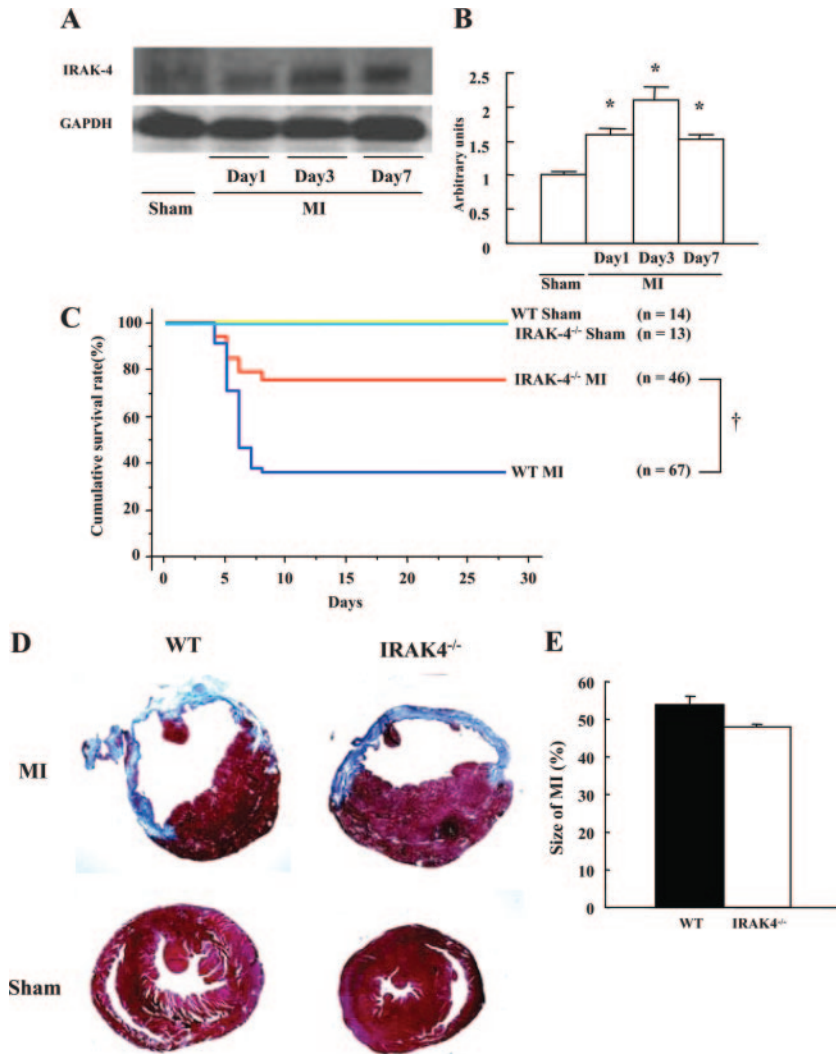


Figure 1. A and B, Western blot and quantification of IRAK-4 in the infarcted myocardium. GAPDH is shown as a loading control. Sham represents data obtained 3 days after sham operation. C, Kaplan–Meier survival analysis. Percentages of surviving WT and IRAK-4^{-/-} mice after sham operation or MI were plotted. Between-group difference was tested by the log-rank test. D, Masson trichrome staining of cardiac sections in WT and IRAK-4^{-/-} mice at 28 days after sham operation or MI. Blue staining indicates fibrosis. E, Infarct size determined with Masson trichrome staining sections. Infarct size values are from WT (n=14) and IRAK-4^{-/-} (n=12) mice surviving at 28 days after MI. *P<0.05 vs sham; †P<0.05 vs WT MI.

Reduced Infiltration of Leukocytes, CD3⁺ T Lymphocytes, and CD11c⁺ DCs into the Injured Myocardium of IRAK-4^{-/-} Mice

On day 3, CD45⁺ leukocyte infiltration into the infarcted site was reduced in IRAK-4^{-/-} mice compared with WT mice. Interestingly, fewer CD3⁺ T lymphocytes and CD11c⁺ DCs were also observed in the infarcted myocardium of IRAK-4^{-/-} compared with WT mice (Figure 2A through 2C). Infiltrating Mac-3⁺ macrophages also tended to be fewer in IRAK-4^{-/-} than in WT mice. In contrast, infiltration of neutrophils into the infarcted portion was similar between WT and IRAK-4^{-/-} mice (Figure 2A and 2C). The number of infiltrating CD3⁺ T-lymphocytes expressing CD154 (one of the activation markers of T lymphocytes) into the infarcted heart tended to be lower in IRAK-4^{-/-} mice than in WT mice (Figure 1A and 1B of the online-only Data Supplement).

Apoptosis Was Attenuated in IRAK-4^{-/-} Mice After MI

The number of apoptotic nuclei as detected by terminal deoxynucleotidyl transferase–mediated dUTP nick-end labeling (TUNEL) staining was significantly lower in the LV border zone of IRAK-4^{-/-} mice compared with WT mice on

day 3 after MI (Figure 2D and 2E). There was no significant difference in the expression of total caspase-3 between WT and IRAK-4^{-/-} mice; however, the expression of cleaved caspase-3 from the LV border zone was significantly reduced in IRAK-4^{-/-} mice compared with WT mice on day 3 after MI (Figure 2F and 2G).

Evidence of Fibrosis on Histological Sections

Collagen volume fraction in the noninfarcted zone based on picrosirius red staining was significantly lower in IRAK-4^{-/-} compared with WT mice at 28 days after MI. Fibrosis in the infarcted region tended to be lower in IRAK-4^{-/-} than WT mice (Figure 3A and 3B).

Inducible Nitric Oxide Synthase Expression in the Injured Myocardium

Inducible nitric oxide (NO) synthase (iNOS) can be upregulated in the ischemic myocardium as part of the innate immune response to tissue injury. iNOS expression and total NO production was attenuated in IRAK-4^{-/-} compared with WT mice after MI (Figure 4A through 4C).

Table. Echocardiographic Analysis, Hemodynamic Analysis, Body Weight, and Ratios of Heart Weight and Lung Weight to Body Weight

	WT Sham	IRAK-4 ^{-/-} Sham	WT MI	IRAK-4 ^{-/-} MI
Echocardiography				
n	5	5	13	14
HR, bpm	465±21	460±20	485±34	490±16
LVEDD, mm	3.32±0.21	3.25±0.19	5.16±0.19*	4.79±0.10*
LVESD, mm	1.77±0.19	1.75±0.16	4.18±0.17*	3.65±0.17*†
FS, %	46.8±2.7	46.1±2.9	19.0±2.3*	23.8±2.8*†
Hemodynamic data				
n	4	4	10	8
LVESP, mm Hg	100±9	105±6	82±5*	91±4*†
dP/dtmax, mm Hg/s	8224±1196	8078±656	6052±337*	7175±1025*†
dP/dtmin, mm Hg/s	-6783±950	-7345±564	-5370±359*	-6031±205*
Organ weight				
n	8	8	10	10
BW (baseline), g	24.2±0.8	24.5±1.1	25.4±0.6	24.7±0.4
BW (day 7), g	27.5±0.9	26.9±1.5	26.7±1.8	25.1±1.3
BW (day 28), g	28.1±1.6	27.8±1.1	28.0±0.8	27.4±1.2
HW/BW (day 7), mg/g	4.63±0.25	4.59±0.34	6.41±0.37*	5.76±0.32*
HW/BW (day 28), mg/g	4.93±0.09	4.85±0.13	6.90±0.43*	5.88±0.37*†
LW/BW (day 7), mg/g	4.63±0.14	4.23±0.40	6.01±0.15*	5.44±0.19*
LW/BW (day 28), mg/g	4.79±0.15	4.59±0.11	6.51±0.31*	5.94±0.36*

HR indicates heart rate; LVEDD, LV end-diastolic dimension; LVESD, LV end-systolic dimension; FS, fractional shortening; LVESP, LV end-systolic pressure; BW, body weight; HW, heart weight; and LW, lung weight.

* $P < 0.05$ vs sham of the same genotype; † $P < 0.05$ vs WT MI.

Defective IRAK-4 Showed Less Phosphorylation of Inhibitor- κ B α , NF- κ B p65, and c-Jun NH2-Terminal Kinase in the Infarcted Myocardium

IRAK-4 is an integral part of TIR signaling activation, which results in NF- κ B activation. NF- κ B activation occurs through the phosphorylation and degradation of inhibitor- κ B ($I\kappa$ B) α , a protein that binds and retains NF- κ B in the cytoplasm of resting cells. Phosphorylated inhibitor- κ B kinase (IKK) α and IKK β protein expression, the 2 catalytic subunits of IKK important for phosphorylation of $I\kappa$ B α , was significantly increased in the infarcted site in WT mice after MI. Phosphorylation and degradation of $I\kappa$ B α and phosphorylation of NF- κ B p65 were induced in WT mice but were significantly suppressed in IRAK-4^{-/-} mice (Figure 5A and 5B). The NF- κ B-DNA binding activity was attenuated in IRAK-4^{-/-} compared with WT mice after MI (Figure 5C). Gene expression of proinflammatory and Th1 cytokines such as IL-1 β , IL-6, TNF- α , and IL-12 was dramatically decreased in IRAK-4^{-/-} mice after MI (Figure 5D). TIR signaling activation also induces mitogen-activated protein kinase pathway activation. The classic mitogen-activated protein kinase signaling pathway comprises 3 major branches named for their terminal effector kinases: the extracellular signal-regulated protein kinases, the c-Jun NH2-terminal kinases (JNK), and p38. The activation of JNK induced by myocardial ischemia was greatly impaired in IRAK-4^{-/-} mice after MI, whereas phosphorylation of p38 and extracellular signal-regulated protein kinase was not diminished in IRAK-4^{-/-} compared

with WT mice (Figure 5E and 5F). These results suggest that IRAK-4 is also critical for the activation of JNK in the TIR signaling after MI.

Difference in Characteristics Between Cardiac DCs From WT and IRAK-4^{-/-} Mice After MI

To further investigate the link between the better survival rate and cardiac function in IRAK-4^{-/-} mice with differential inflammatory cell mobilization, we focused on the difference in characteristics of DCs between WT and IRAK-4^{-/-} mice. The number of DCs in the peripheral circulation increased and peaked 3 days after MI in WT mice (Figure 6A). DCs can reside in the noninflamed heart, and the population of DCs in the infarcted myocardium expands after MI. Although our data confirmed that there are some DCs in the heart under resting conditions (0.16%), surprisingly, the DC population in the heart after MI expanded very significantly to 3.66% (Figure 6B through 6D). However, this was reduced in the IRAK-4^{-/-} hearts. Light microscopy also showed morphological changes in DCs from WT mice after MI compared with after sham operation (Figure 6E). Expression of CD80 and CD86, which are DC maturation markers, was much higher in WT- than IRAK-4^{-/-}-derived cardiac DCs after MI. Similarly, cytokine gene expression such as IL-6, TNF- α , IL-12a, and IL-12b markedly increased in WT but not in IRAK-4^{-/-} cardiac DCs (Figure 6F). These findings suggest that in contrast to WT-derived cardiac DCs, IRAK-4^{-/-} cardiac DCs have an impaired maturation process after ischemia and a decreased ability to produce proinflammatory and Th1 cytokines.

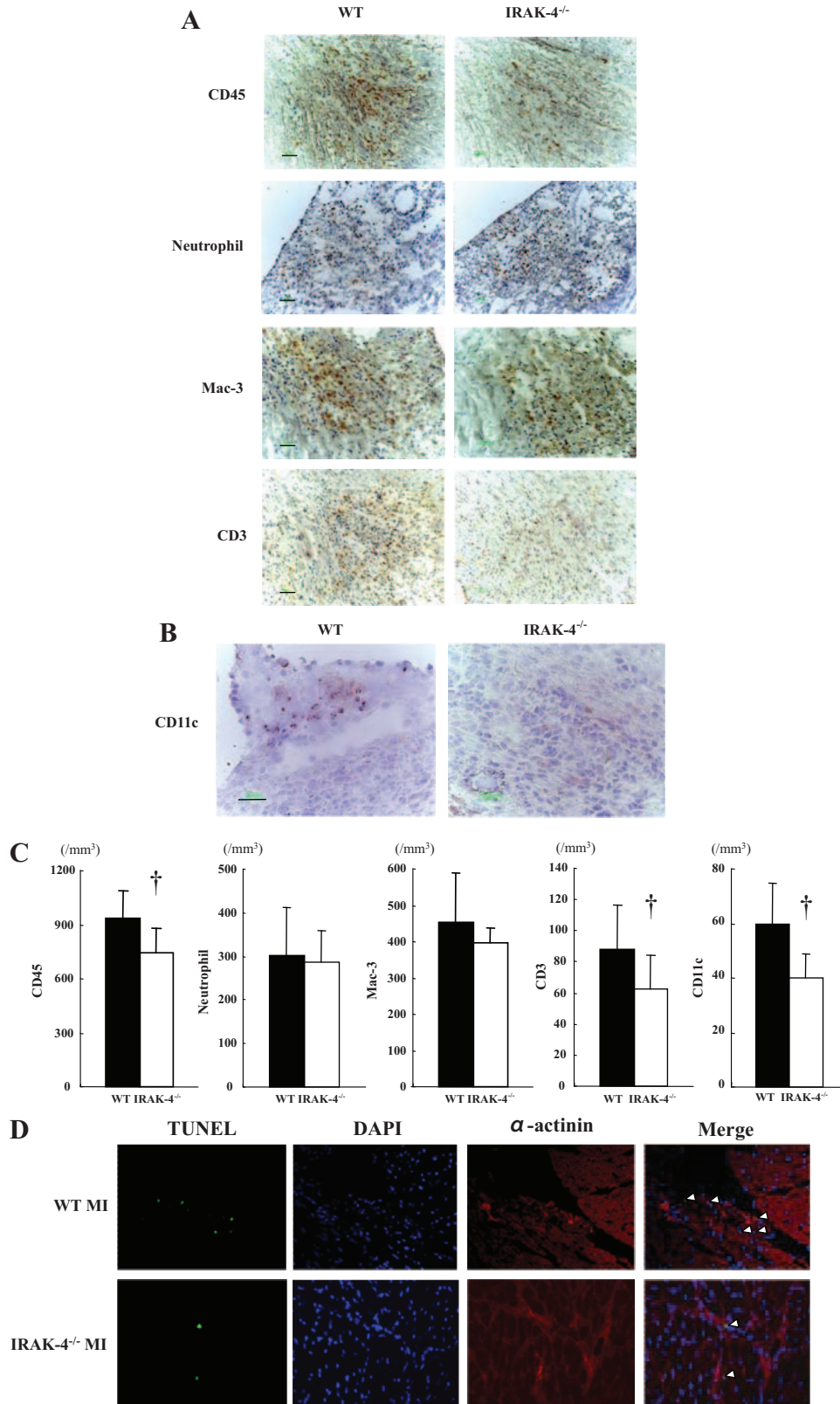


Figure 2. A and B, Infiltration of CD45⁺ leukocytes, neutrophils, Mac-3⁺ macrophages, CD3⁺ T lymphocytes, and CD11c⁺ DCs into the infarcted hearts of WT and IRAK-4^{-/-} mice. Scale bar=50 μ m. C, Numbers of CD45⁺ leukocytes, neutrophils, Mac-3⁺ macrophages, CD3⁺ T lymphocytes, and CD11c⁺ DCs. D, Representative LV sections demonstrating TUNEL-positive nuclei (marked by white arrows) in the border zone of WT and IRAK-4^{-/-} mice on day 3 after MI. Cardiomyocytes were visualized by an anti- α -actinin antibody (red). E, Number of TUNEL-positive nuclei in MI-operated WT and IRAK-4^{-/-} mice (n=4 per group). F, Representative immunoblot analysis of the large fragment (17 kDa) of cleaved caspase-3 and uncleaved caspase-3 (35 kDa) in the infarcted myocardium of WT and IRAK-4^{-/-} mice on day 3 after MI. G, Results of quantitative analysis of cleaved caspase-3 (n=5 per group). **P*<0.05 vs sham; †*P*<0.05 vs WT MI.

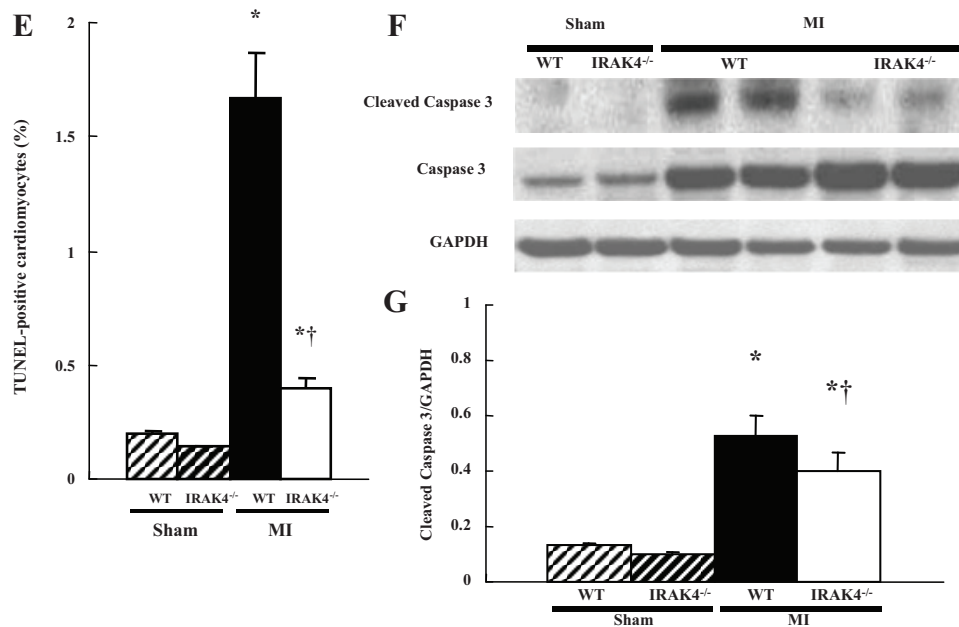


Figure 2. (Continued).

Characteristics of BMDCs From WT and IRAK-4^{-/-} Mice

To further characterize the mobilized DCs after MI, we compared BMDCs from WT and IRAK-4^{-/-} mice in response to several endogenous ligands. Expression of CD80, CD86, and major histocompatibility complex class II, which are DC maturation markers, increased in BMDCs of WT mice after lipopolysaccharide stimulation, but this was blunted in IRAK-4^{-/-} mice. On the other hand, heat shock protein (HSP)-70, an endogenous ligand for TIR signaling, did not upregulate these markers on BMDCs in either WT or IRAK-4^{-/-} mice (Figure 7A and 7B). BMDCs from WT mice showed robust proinflammatory and Th1 cytokine production to lipopolysaccharide, HSP70, and necrotic cell supernatants from HL-1 (cardiomyocytes) and mouse embryonic fibroblasts containing HSP70 (Figure 7D), but BMDCs from IRAK-4^{-/-} mice displayed a markedly blunted cytokine production and gene expression (Figure 7C and 7E). These findings suggest that HSP70 induced not phenotypic but functional DC maturation. Additionally, using several strategies, including addition of polymyxin B to the culture medium and heat inactivation of the recombinant protein, we confirmed that *in vitro* observations were attributable to the actions of HSP70 and not contaminants such as lipopolysaccharide. Mature DCs not only can produce more cytokines but also can induce T-lymphocyte proliferation. Compared with WT-derived BMDCs, IRAK-4^{-/-}-derived BMDCs have less ability to proliferate allogeneic CD4⁺ T lymphocytes (Figure 7F). Taken together, BMDCs from IRAK-4^{-/-} mice have less ability to produce cytokines in response to endogenous ligands of TIR and to proliferate T lymphocytes compared with BMDCs from WT mice.

IRAK-4^{-/-} DCs Have Less Mobilization Capacity *In Vivo*

To compare IRAK-4^{-/-} DC with WT DC mobilization capacity *in vivo*, we analyzed mobilized DCs in the spleen

after cytokine treatment. The number of CD11c⁺CD11b⁺ DCs was significantly lower in the spleen of IRAK-4^{-/-} mice compared with WT mice on day 7 after cytokine treatment, although the number of CD11c⁺CD11b⁺ DCs in the spleen was similar between WT and IRAK-4^{-/-} mice after PBS treatment (Figure 7G and 7H). These findings indicate that IRAK-4^{-/-} myeloid DCs have less mobilization capacity *in vivo* compared with WT myeloid DCs.

IRAK-4^{-/-} BMDCs Have Less Migration Ability

To clarify the mechanism of the difference in DC migration between WT and IRAK-4^{-/-} mice, we evaluated chemokine expression in the infarcted heart and DC migration to DC-related chemokines. Chemokine (C-C motif) ligand 5 (CCL5) expression in the infarcted heart was lower in IRAK-4^{-/-} mice (Figure II of the online-only Data Supplement). IRAK-4^{-/-} BMDCs have less migration ability in response to macrophage inflammatory protein-1 α and -1 β , CCL2, and CCL5 (Figure III of the online-only Data Supplement). These results revealed that decreased CCL5 expression in the heart and an impaired migratory capacity of IRAK-4^{-/-} BMDCs in response to DC-related chemokines contribute to less DCs migration into the infarcted heart.

Adoptive Transfer of BMDCs From WT to IRAK-4^{-/-} Mice

Our data indicate that the failure to induce proinflammatory and Th1 cytokine production in IRAK-4^{-/-} DCs is due in part to defective functional DC maturation. To prove that this is the key factor affecting survival rate and the remodeling process after MI, we performed an adoptive transfer experiment using WT DCs. Transfer of WT-derived BMDCs into IRAK-4^{-/-} mice negated entirely the survival advantage observed with IRAK-4^{-/-} mice during the 4-week follow-up after MI (IRAK-4^{-/-} without WT-derived BMDCs, 76%; IRAK-4^{-/-} with WT-derived BMDCs, 33%; Figures 1C and

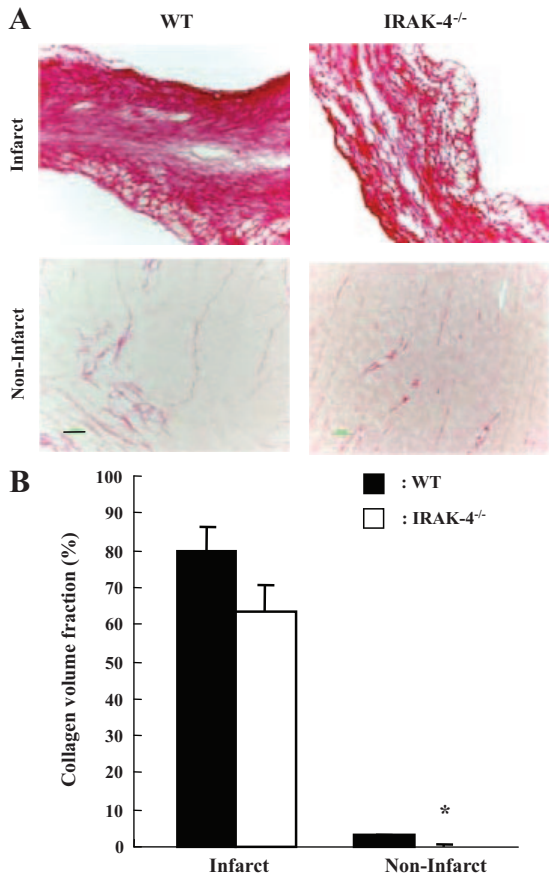


Figure 3. A, Representative photographs of picosirius red-stained infarcted and noninfarcted myocardium of WT and IRAK-4^{-/-} mice. Scale bar=50 μm. B, Collagen volume fraction of MI from WT and IRAK-4^{-/-} mice (n=10 per group). †P<0.05 vs WT MI.

8A). In contrast, the survival rate of WT recipient mice was not altered after transfer (WT without WT-derived BMDCs, 36%; WT with WT-derived BMDCs, 31%; Figures 1C and 8A). All sham-operated mice with BMDCs survived during the 4 weeks after MI. CFSE-labeled DCs were distributed equally in the heart of WT and IRAK-4^{-/-} mice after transfer (Figure 8B). To evaluate the influence of procedures themselves on results, we also performed PBS injection into WT or IRAK-4^{-/-} mice after MI. The survival rate was similar between WT or IRAK-4^{-/-} mice with PBS injection and without injection after MI (Figures 1C and 8A). The survival rate of IRAK-4^{-/-} recipient mice was unchanged after transfer of IRAK-4^{-/-}-derived BMDCs (Figure 8A). In addition to the decrease in survival rate, there was no significant difference in the ratio of heart weight to body weight between WT and IRAK-4^{-/-} mice after the transfer of WT-derived BMDCs, although the ratio of heart weight to body weight in IRAK-4^{-/-} mice was smaller than in WT mice at 28 days after MI (the Table and Figure 8C). The LV end-systolic dimension and fractional shortening were also comparable between WT and IRAK-4^{-/-} mice after the transfer of WT-derived BMDCs at 28 days after MI (Figure 8D). These results indicated that DCs themselves can influence survival rate and cardiac morphology through modulating the inflammatory process after MI.

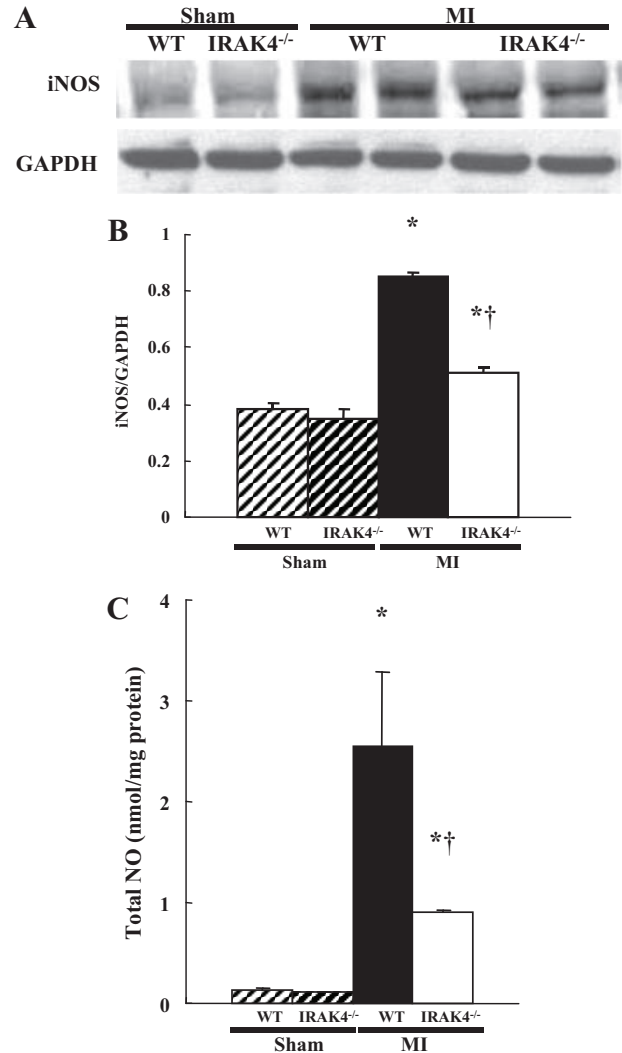


Figure 4. A and B, Representative immunoblots and the results of quantitative analysis for iNOS in the hearts of WT and IRAK-4^{-/-} mice after sham operation or MI (n=4 per group). C, NO production in the infarcted myocardium of WT and IRAK-4^{-/-} mice after sham operation or MI (n=4 per group). *P<0.05 vs sham; †P<0.05 vs WT MI.

Discussion

The present study demonstrated that IRAK-4^{-/-} mice had a higher survival rate and improved function and remodeling through decreased inflammation resulting from the blunted innate immune response after MI. This was mediated mainly through the inability of BMDCs to mobilize, mature, and produce cytokines in the IRAK-4^{-/-} mice. The adoptive transfer of WT-derived mature BMDCs into IRAK-4^{-/-} mice decreased the survival advantage and worsened the cardiac remodeling of IRAK-4^{-/-} mice after MI such that they were indistinguishable from WT controls. This finding suggests that the innate immune system activation and IRAK-4 signaling were crucial for BMDC mobilization and maturation, contributing to post-MI mortality and adverse remodeling.

Inflammatory response and cytokine elaboration play a particularly active role after MI; in turn, the degree of the inflammatory response is an important determinant of the outcome of the host.¹⁵ In IRAK-4^{-/-} mice, attenuation of TIR

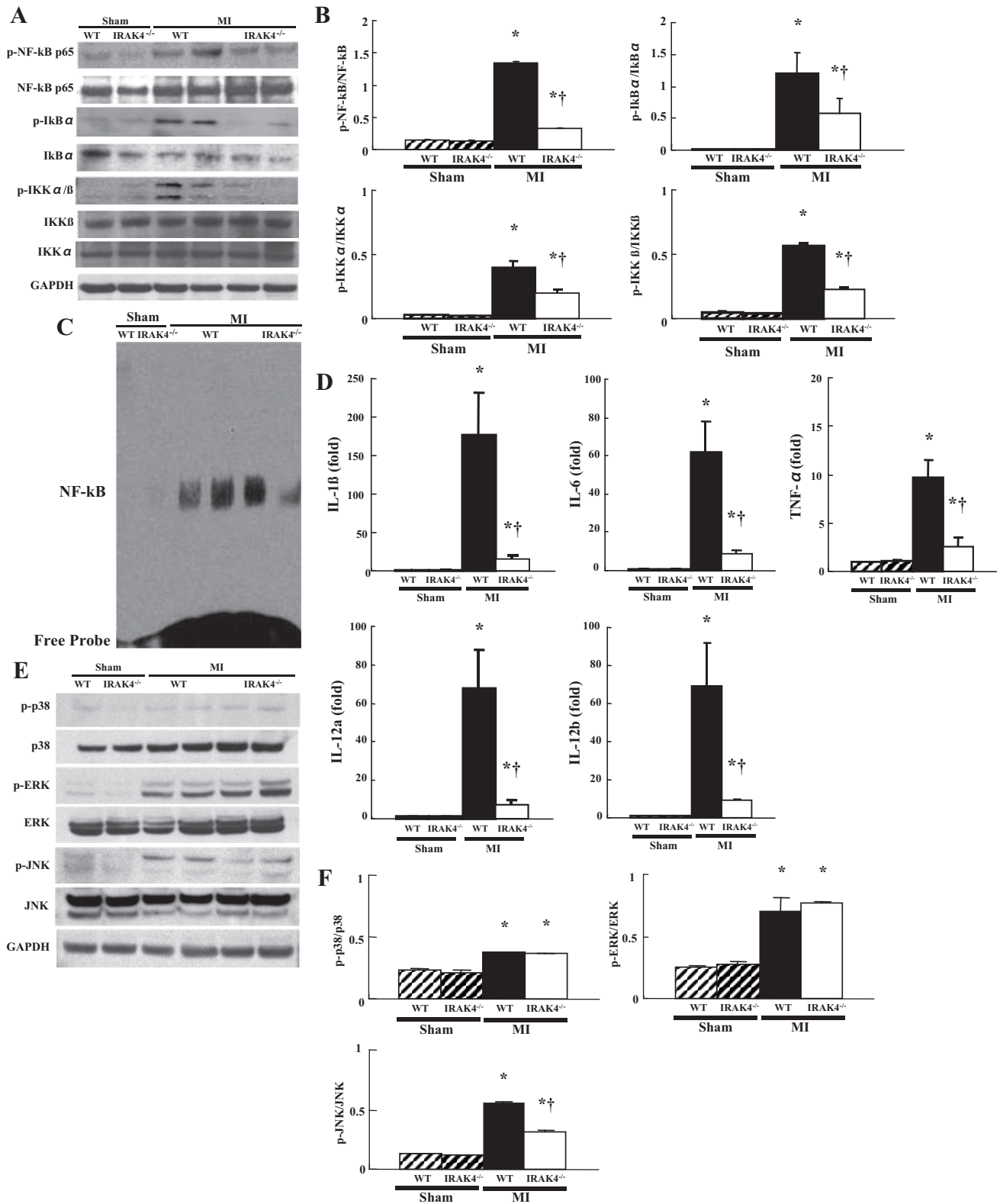


Figure 5. A and B, Representative immunoblots and the results of quantitative analysis of IKK α , IKK β , I κ B α , and NF- κ B p65 expression in the infarcted heart (n=4 per group). C, NF- κ B-DNA binding activity in the infarcted myocardium of WT and IRAK-4^{-/-} mice was determined by electrophoretic mobility shift assay (n=4 per group). D, Expression of various cytokine genes in the infarcted myocardium of WT and IRAK-4^{-/-} mice (n=10 per group). The amounts of target mRNAs were normalized to 18S rRNA levels. E and F, Representative immunoblots and the results of quantitative analysis of mitogen-activated protein kinase expression in the infarcted heart of WT and IRAK-4^{-/-} mice (n=4 per group). *P<0.05 vs sham; †P<0.05 vs WT MI.

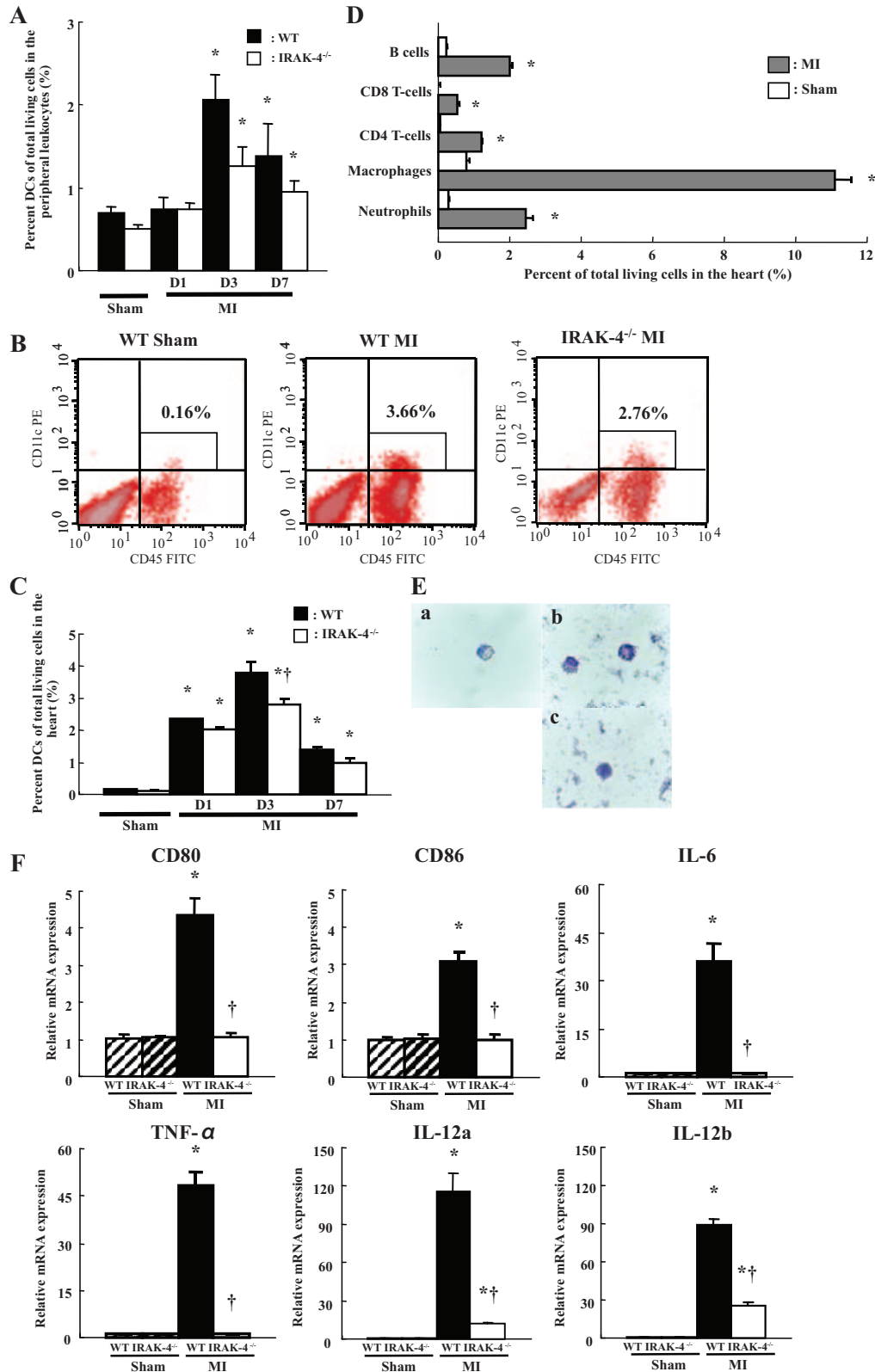


Figure 6. A, Percentage of DCs in peripheral leukocytes of WT mice subjected to sham or MI. Similar results were obtained in 3 independent experiments. B, Flow cytometric assessment of heart-infiltrating DCs. Representative dot plots of CD45-FITC/CD11c-PE profile of WT and IRAK-4^{-/-} mice 3 days after sham operation or MI. Numbers on the plots indicate the percentage of CD11c⁺ DCs of CD45⁺ leukocytes. C, Percentage of DCs in the infarcted hearts of WT and IRAK-4^{-/-} mice subjected to sham or MI. D, Analysis of non-CD11c⁺ cell population from digested WT sham-operated or MI hearts on day 3 by flow cytometry. E, Representative Wright Giemsa staining of individual DCs from sham-operated or MI heart suspensions in WT and IRAK-4^{-/-} mice. a, WT sham; b, WT MI; c, IRAK-4^{-/-} MI. F, Cytokines and maturation markers of mRNA expression in DCs from heart suspensions 3 days after sham operation or MI in WT and IRAK-4^{-/-} mice. **P*<0.05 vs sham; †*P*<0.05 vs WT MI.

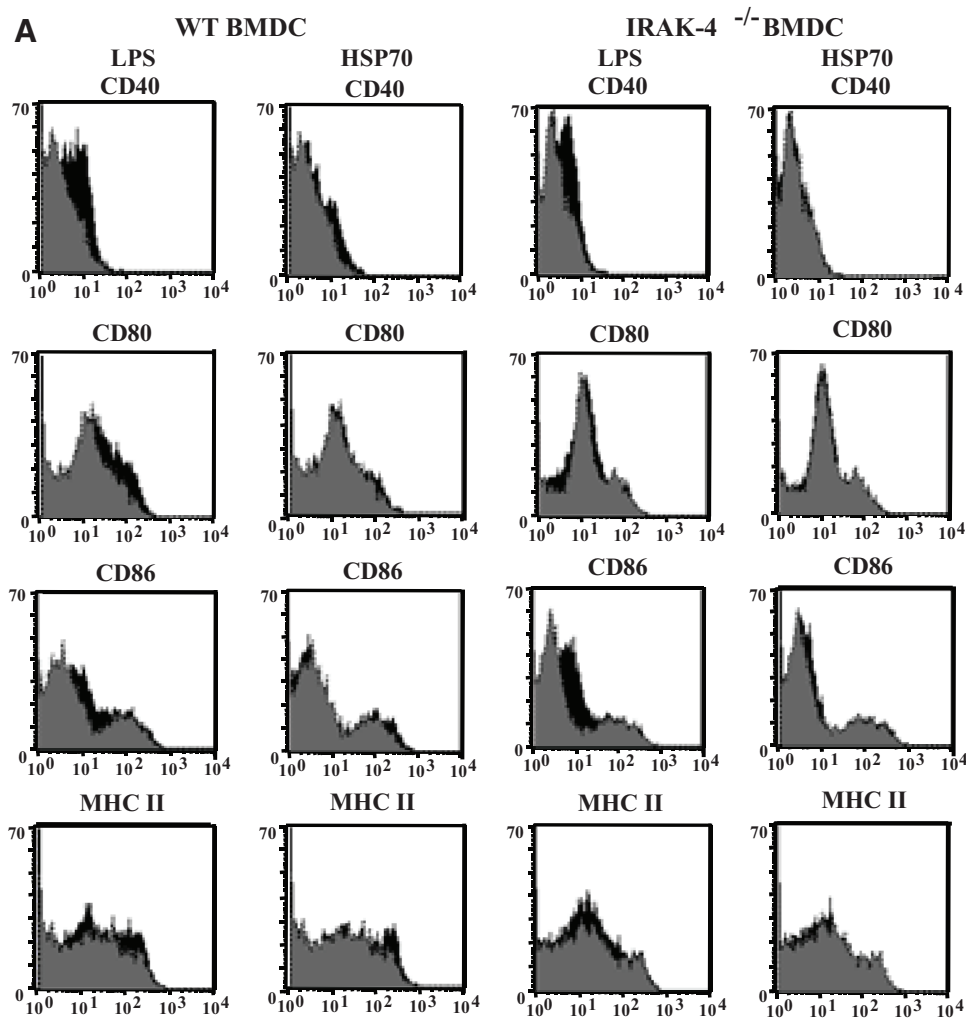


Figure 7. A and B, Analysis of BMDC maturation after exposure to lipopolysaccharide (LPS) or HSP70. Gray area indicates no stimulation (NS); black area, LPS or HSP70 stimulation in WT or IRAK-4^{-/-} mice. CD40, CD80, CD86, and major histocompatibility complex class II expression as maturation marker was assessed by flow cytometry. **P*<0.05 vs WT NS. C, Cytokine secretion by BMDCs in response to LPS or HSP70. BMDCs of WT and IRAK-4^{-/-} mice were incubated for 24 hours with 1 μg/mL LPS, 50 μg/mL HSP70, or 50 μg/mL HSP70 with 25 μg/mL polymyxin B (PB) or heat inactivated 50 μg/mL HSP70. **P*<0.05 vs sham; †*P*<0.05 vs WT MI. D, HSP70 in the supernatant of necrotic mouse embryonic fibroblasts (MEFs) or HL-1 was assessed by Western blotting. As a control, recombinant HSP70 (rHSP70; 100 ng per lane) was used. E, Cytokine mRNA expression in BMDCs from WT and IRAK-4^{-/-} mice without treatment (NS) or after treatment with supernatant of necrotic cells after freeze-thaw lysis. **P*<0.05 vs WT NS; †*P*<0.05 vs WT HL-1 or MEFs. F, To assess T-cell proliferation in response to allogeneic prestimulated BMDCs, we measured loss of incorporated CFSE labeling by flow cytometric analysis, resulting in cells with lower levels of fluorescence of CFSE. To detect helper T cells, we performed a dual staining together with PE-labeled CD4 antibodies. (G) Representative dot plots of CD11c-FITC/CD11b-PE profile of WT and IRAK-4^{-/-} mice 7 days after the combination of granulocyte macrophage colony-stimulating factor/stromal cell-derived factor-1 (GM-CSF/SDF-1) treatment. Numbers on the plots indicate the percentage of CD11c⁺CD11b⁺ DCs (myeloid DCs) of total living cells in the spleen. H, Percentage of CD11c⁺CD11b⁺ DCs in the spleen of WT and IRAK-4^{-/-} mice after PBS or GM-CSF/SDF-1 treatment (n=3 to 5). MFI indicates mean fluorescent intensity. **P*<0.05 vs WT.

signaling resulted in lower expression of cytokines and decreased inflammation through blunted innate immune response. Previous reports suggested that proinflammatory cytokines induce cardiomyocyte apoptosis and cardiac fibrosis and positively correlate with iNOS expression.^{16,17} Consistent with these findings, the present study demonstrated increased cardiomyocyte apoptosis and cardiac fibrosis in the noninfarcted myocardium and higher iNOS expression and elevated total NO production in WT but not IRAK-4^{-/-} mice.

NF-κB is a key transcription factor that regulates inflammatory processes and greatly contributes to the pathophysiology of MI. Inhibition of NF-κB by a knockout model and

pharmacological approach showed improvement in survival and cardiac function after MI.^{18,19} Consistent with those studies, we showed attenuation of NF-κB activity in IRAK-4^{-/-} mice, which was associated with lower proinflammatory and Th1 cytokine gene expression and thus better a survival rate and hemodynamics after MI. On the other hand, a previous study showed that NF-κB protects the adult cardiac myocyte against myocardial ischemia.²⁰ Dichotomous findings reflect the overall experimental design itself, which highlights the complexity intrinsic to NF-κB signaling pathways and their dependency on specific conditions. However, our results showed that not only NF-κB but also JNK activation was severely impaired in

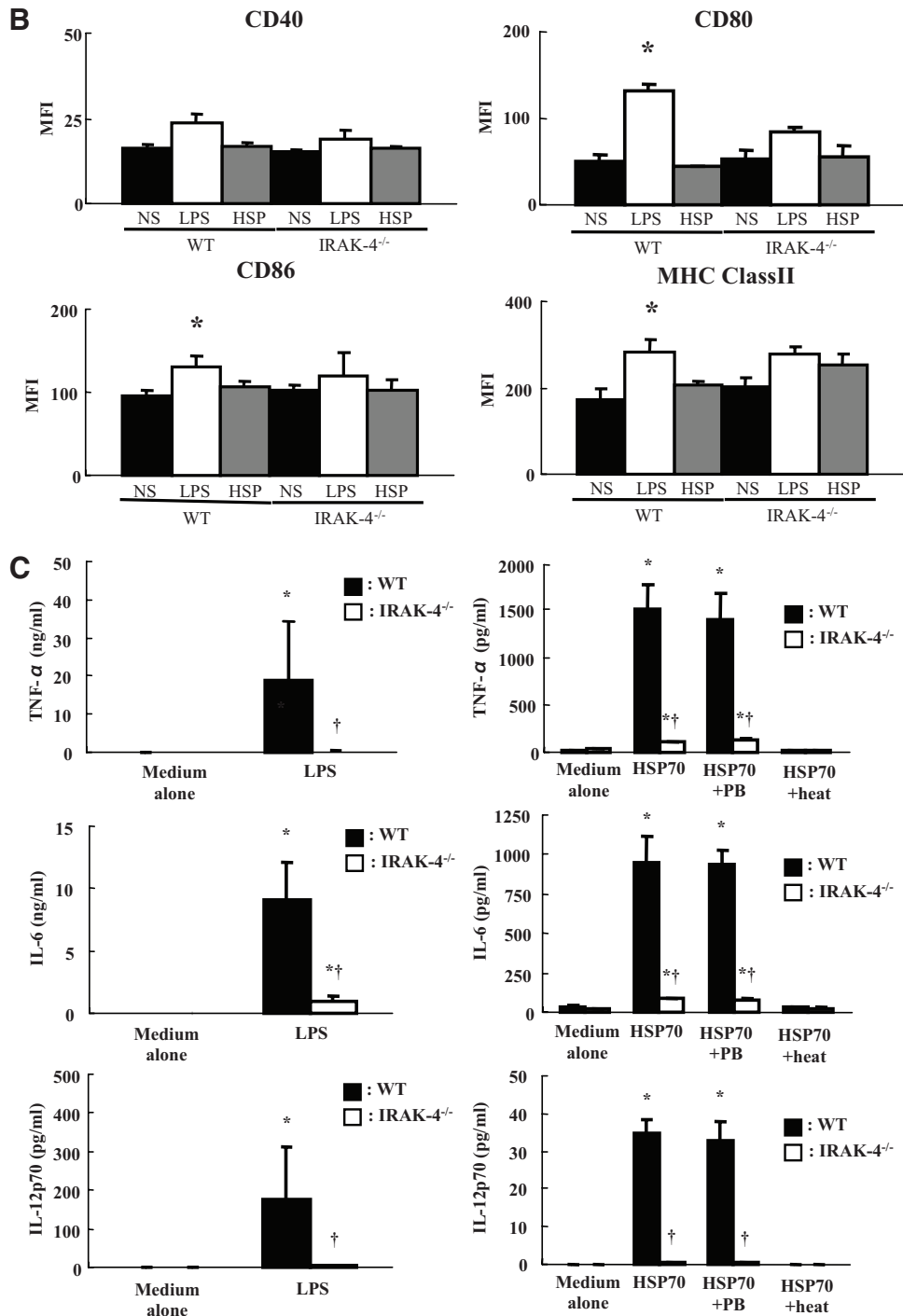


Figure 7. (Continued).

IRAK-4^{-/-} mice after MI. JNK is also activated after MI, and inhibition of JNK inhibits IL-6 transcription.²¹ Accordingly, we provide evidence that the attenuation of NF- κ B and JNK activity in IRAK-4^{-/-} mice resulted in decreased inflammation and thus improved host outcome after MI.

In our study, HSP70, which is one of the endogenous ligands, was highly expressed in the infarcted heart (data not shown), and cardiac DCs showed upregulation of IL-1 β , IL-6, TNF- α , and IL-12 in WT mice after MI. It is tempting to speculate that in response to the danger signal HSP70

released by necrotic myocardium, cardiac DCs become activated and can upregulate proinflammatory and Th1 cytokine expression. Our in vitro results showed that BMDCs from WT mice produced a significant amount of inflammatory cytokines in response to HSP70 and necrotic cell supernatants. Importantly, the present in vitro results are consistent with several studies that have shown that HSP70 activates BMDCs and induces proinflammatory and Th1 cytokine production through the activation of TLR2 and TLR4 signaling and that dying cells can activate DCs, thus causing “sterile

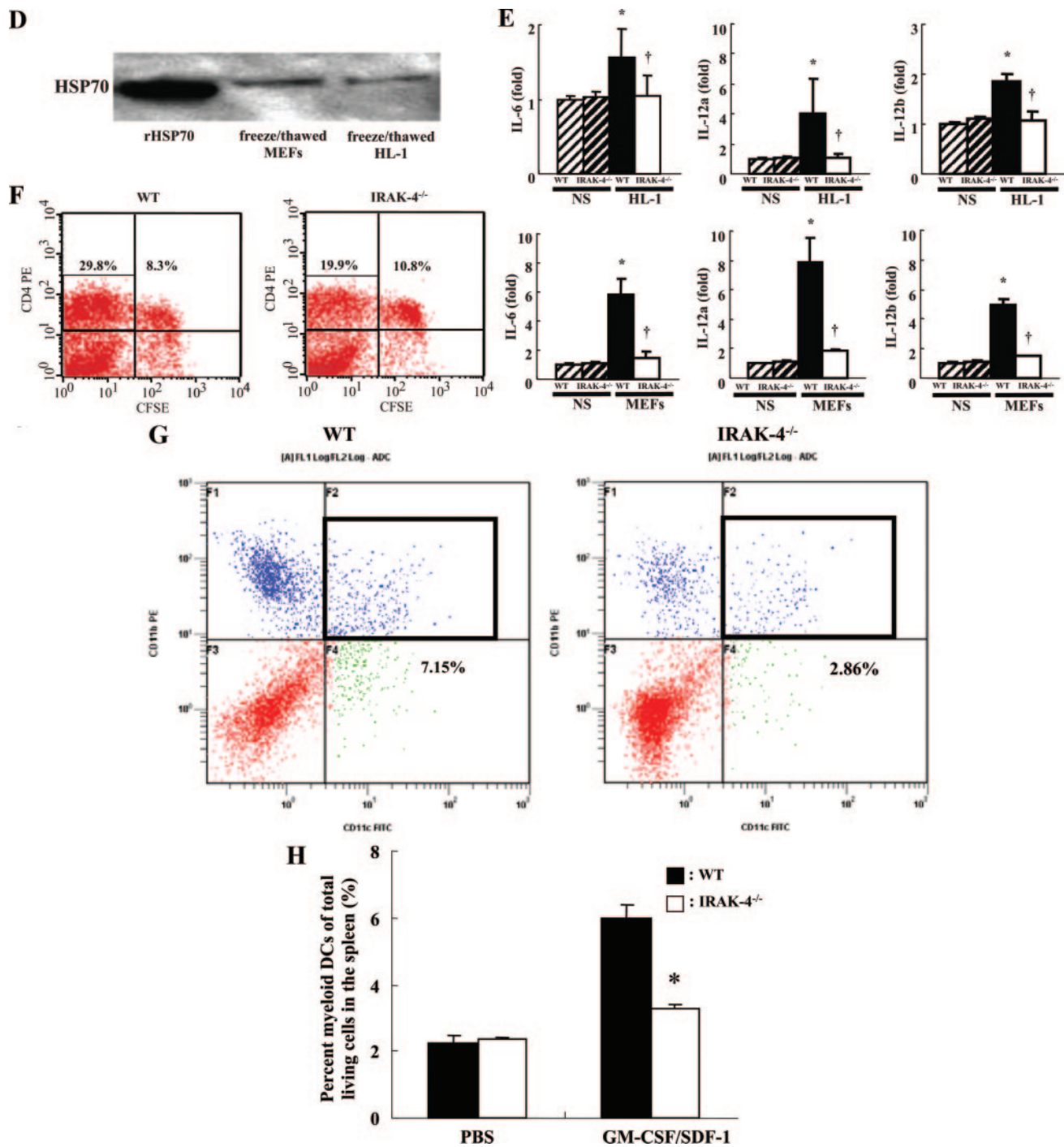


Figure 7. (Continued).

inflammation.²²⁻²⁴ In contrast, BMDCs from IRAK-4^{-/-} mice were severely impaired in their ability to produce proinflammatory and Th1 cytokines. Furthermore, IRAK-4^{-/-} DCs have less mobilization capacity in vivo, which is closely associated with the reduced number of DCs infiltrating into the infarcted heart in IRAK-4^{-/-} mice. These results suggest that deficiency in IRAK-4 led to not only reduced DC mobilization but also a blunted response in mobilized BMDCs when triggered with the endogenous ligands and thus prevented DC activation under myocardial ischemia.

DCs constitutively express cardiac self-antigens on major histocompatibility complex class II molecules even in the normal heart,²⁵ and some patients have cardiac-specific autoimmune response after MI.²⁶ Furthermore, Göser et al²⁷ showed that mice preimmunized with murine cardiac troponin I displayed greater infarct size, more fibrosis, higher inflammation score, and cardiac dysfunction after MI. These findings indicate that myocardial damage results in release of not only endogenous ligands of TLRs but also self-antigens. If self-antigen-loaded DCs become activated via TLR stim-

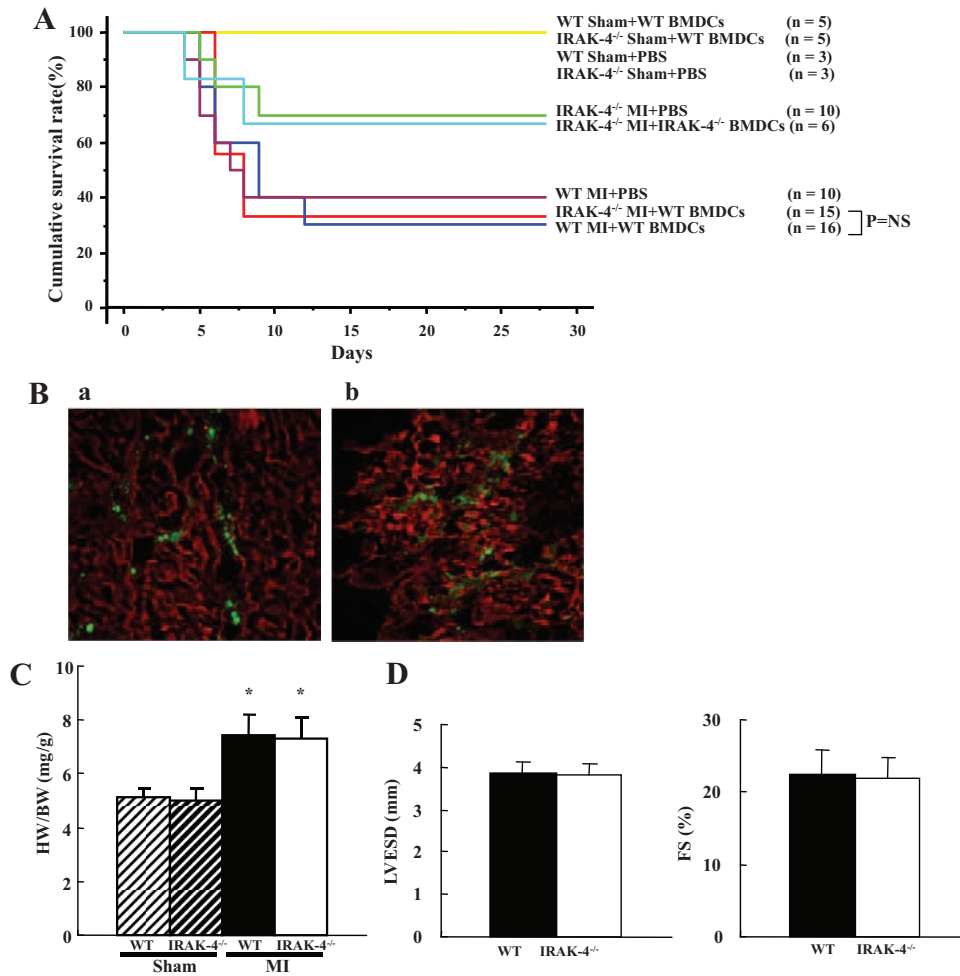


Figure 8. DCs from WT functional reconstitution in vivo. A, Kaplan–Meier survival analysis after adoptive transfer. Percentages of surviving WT and IRAK-4^{-/-} mice treated with BMDCs from WT mice, BMDCs from IRAK-4^{-/-} mice, or PBS after sham operation or MI were plotted. Between-group difference was tested by the log-rank test. B, Representative immunofluorescence images showing the distribution of CFSE-labeled BMDCs after injection in the infarcted myocardium of WT (a) and IRAK-4^{-/-} (b) mice. Cardiomyocytes were visualized with anti- α -actinin antibody (red). C, Assessment of heart weights (HW) normalized to body weights (BW) after adoptive transfer at 28 days after sham operation or MI (n=5 per group). D, LV end-systolic dimension (LVESD) and fractional shortening (FS) after adoptive transfer at 28 days after MI (n=5 per group). *P<0.05 vs sham.

ulation by endogenous ligands after MI, this might be sufficient for the initiation of an autoimmune response. Several studies showed that activated T lymphocytes infiltrate into infarcted and noninfarcted myocardium after MI.^{26,28} DC activation mediated by TLRs and thereafter direct interaction between activated DCs and T lymphocytes are required before T-lymphocyte activation. Yang et al²⁹ showed that CD4⁺ T lymphocytes are activated early during reperfusion and contribute to an early inflammatory response in myocardial reperfusion injury. These findings support our results that CD80 and CD86 are expressed on cardiac DCs upregulated in WT mice after MI because CD80 and CD86 upregulation is required for activation of naïve T lymphocytes.⁷ In IRAK-4^{-/-} mice, cardiac DCs had lower expression of CD80 and CD86 genes after MI and BMDCs had less ability to proliferate CD4⁺ T lymphocytes, indicating that decreased inflammation in the infarcted myocardium of IRAK-4^{-/-} mice may be associated with decreased T-lymphocyte activation. Unlike autoimmune myocarditis, further investigation is needed to determine to what extent

autoimmune response contributes to the inflammatory process after MI, although autoreactive CD3⁺ T lymphocytes were observed and Th1 not Th17 T-cell response was predominant in our model (data not shown). However, autoimmunity may be one of the possible mechanisms by which DCs affect the inflammatory process after MI, and some clinical and experimental observations support this mechanism.^{26,30,31}

Conclusions

The present findings are the first to demonstrate a critical role for IRAK-4 in survival and cardiac remodeling and the importance of DCs in the inflammatory process after MI. IRAK-4 could be a potential target for the treatment of patients with post-MI heart failure.

Acknowledgments

We would like to thank Dr Takahiro Nonaka for technical assistance and critical reading of the manuscript and Dr Peter Zandstra for advice and comments.

Sources of Funding

This study was supported by research grants from the Canadian Institutes of Health Research, Genome Canada, and the Heart and Stroke Foundation of Ontario. Dr Liu is the Scientific Director of the Institute of Circulatory and Respiratory Health of CIHR and holds the Heart and Stroke/Polo Chair Professorship at University of Toronto. Dr Maekawa received a postdoctoral fellowship from AstraZeneca and the Heart and Stroke Foundation of Canada, Tailored Advanced Collaborative Training in Cardiovascular Science, and Japan Heart Foundation/Bayer Yakuhin Research Grant Abroad.

Disclosures

Dr Yeh currently is a research leader at Amgen Inc, and Dr Suzuki is a researcher at Takeda Pharmaceuticals. Both collaborated in this project because of their internationally recognized expertise in innate immunity. There are no conflicts of interest with respect to this specific study. The other authors report no conflicts.

References

- Matzinger P. The danger model: a renewed sense of self. *Science*. 2002;296:301–330.
- Fuse K, Chan G, Liu Y, Gudgeon P, Husain M, Chen M, Yeh WC, Akira S, Liu PP. Myeloid differentiation factor-88 plays a crucial role in the pathogenesis of Coxsackievirus B3-induced myocarditis and influences type I interferon production. *Circulation*. 2005;112:2276–2285.
- Marty RR, Dirnhofer S, Mauermann N, Schweikert S, Akira S, Hunziker L, Penninger JM, Eriksson U. MyD88 signaling controls autoimmune myocarditis induction. *Circulation*. 2006;113:258–265.
- Shishido T, Nozaki N, Yamaguchi S, Shibata Y, Nitobe J, Miyamoto T, Takahashi H, Arimoto T, Maeda K, Yamakawa M, Takeuchi O, Akira S, Takeishi Y, Kubota I. Toll-like receptor-2 modulates ventricular remodeling after myocardial infarction. *Circulation*. 2003;108:2905–2910.
- Akira S, Takeda K. Toll-like receptor signalling. *Nat Rev Immunol*. 2004;4:499–511.
- Suzuki N, Suzuki S, Yeh WC. IRAK-4 as the central TIR signaling mediator in innate immunity. *Trends Immunol*. 2002;23:503–506.
- Banchereau J, Steinman RM. Dendritic cells and the control of immunity. *Nature*. 1998;392:245–252.
- Lipscomb MF, Masten BJ. Dendritic cells: immune regulators in health and disease. *Physiol Rev*. 2002;82:97–130.
- Banchereau J, Briere F, Caux C, Davoust J, Lebecque S, Liu YJ, Pulendran B, Palucka K. Immunobiology of dendritic cells. *Annu Rev Immunol*. 2000;18:767–811.
- Sallusto F, Lanzavecchia A. Mobilizing dendritic cells for tolerance, priming, and chronic inflammation. *J Exp Med*. 1999;189:611–614.
- Zhang J, Yu ZX, Fujita S, Yamaguchi ML, Ferrans VJ. Interstitial dendritic cells of the rat heart: quantitative and ultrastructural changes in experimental myocardial infarction. *Circulation*. 1993;87:909–920.
- Eriksson U, Ricci R, Hunziker L, Kurrer MO, Oudit GY, Watts TH, Sonderegger I, Bachmaier K, Kopf M, Penninger JM. Dendritic cell-induced autoimmune heart failure requires cooperation between adaptive and innate immunity. *Nat Med*. 2003;9:1484–1490.
- Oyama J, Blais C Jr, Liu X, Pu M, Kobzik L, Kelly RA, Bourcier T. Reduced myocardial ischemia-reperfusion injury in toll-like receptor 4-deficient mice. *Circulation*. 2004;109:784–789.
- Suzuki N, Suzuki S, Duncan GS, Millar DG, Wada T, Mirtsos C, Takada H, Wakeham A, Itie A, Li S, Penninger JM, Wesche H, Ohashi PS, Mak TW, Yeh WC. Severe impairment of interleukin-1 and Toll-like receptor signalling in mice lacking IRAK-4. *Nature*. 2002;416:750–756.
- Nian M, Lee P, Khaper N, Liu P. Inflammatory cytokines and postmyocardial infarction remodeling. *Circ Res*. 2004;94:1543–1553.
- Ing DJ, Zang J, Dzau VJ, Webster KA, Bishopric NH. Modulation of cytokine-induced cardiac myocyte apoptosis by nitric oxide, Bak, and Bcl-x. *Circ Res*. 1999;84:21–33.
- Li HL, Zhuo ML, Wang D, Wang AB, Cai H, Sun LH, Yang Q, Huang Y, Wei YS, Liu PP, Liu DP, Liang CC. Targeted cardiac overexpression of A20 improves left ventricular performance and reduces compensatory hypertrophy after myocardial infarction. *Circulation*. 2007;115:1885–1894.
- Onai Y, Suzuki J, Maejima Y, Haraguchi G, Muto S, Itai A, Isobe M. Inhibition of NF- κ B improves left ventricular remodeling and cardiac dysfunction after myocardial infarction. *Am J Physiol Heart Circ Physiol*. 2007;292:H530–H538.
- Frantz S, Hu K, Bayer B, Gerondakis S, Strotmann J, Adamek A, Ertl G, Bauersachs J. Absence of NF-kappaB subunit p50 improves heart failure after myocardial infarction. *FASEB J*. 2006;20:1918–1920.
- Misra A, Haudek SB, Knuefermann P, Vallejo JG, Chen ZJ, Michael LH, Sivasubramanian N, Olson EN, Entman ML, Mann DL. Nuclear factor-kappaB protects the adult cardiac myocyte against ischemia-induced apoptosis in a murine model of acute myocardial infarction. *Circulation*. 2003;108:3075–3078.
- de Haij S, Bakker AC, van der Geest RN, Haegeman G, Vanden Berghe W, Aarbiou J, Daha MR, van Kooten C. NF-kappaB mediated IL-6 production by renal epithelial cells is regulated by c-jun NH2-terminal kinase. *J Am Soc Nephrol*. 2005;16:1603–1611.
- Millar DG, Garza KM, Odermatt B, Elford AR, Ono N, Li Z, Ohashi PS. Hsp70 promotes antigen-presenting cell function and converts T-cell tolerance to autoimmunity in vivo. *Nat Med*. 2003;9:1469–1476.
- Gallucci S, Lolkema M, Matzinger P. Natural adjuvants: endogenous activators of dendritic cells. *Nat Med*. 1999;5:1249–1255.
- Chen CJ, Kono H, Golenbock D, Reed G, Akira S, Rock KL. Identification of a key pathway required for the sterile inflammatory response triggered by dying cells. *Nat Med*. 2007;13:851–856.
- Donermeyer DL, Beisel KW, Allen PM, Smith SC. Myocarditis-inducing epitope of myosin binds constitutively and stably to I-Ak on antigen-presenting cells in the heart. *J Exp Med*. 1995;182:1291–1300.
- Moraru M, Roth A, Keren G, George J. Cellular autoimmunity to cardiac myosin in patients with a recent myocardial infarction. *Int J Cardiol*. 2006;107:61–66.
- Göser S, Andrassy M, Buss SJ, Leuschner F, Volz CH, Ottl R, Zittrich S, Blaudeck N, Hardt SE, Pfitzer G, Rose NR, Katus HA, Kaya Z. Cardiac troponin I but not cardiac troponin T induces severe autoimmune inflammation in the myocardium. *Circulation*. 2006;114:1693–1702.
- Abbate A, Bonanno E, Mauriello A, Bussani R, Biondi-Zoccai GG, Liuzzo G, Leone AM, Silvestri F, Dobrina A, Baldi F, Pandolfi F, Biasucci LM, Baldi A, Spagnoli LG, Crea F. Widespread myocardial inflammation and infarct-related artery patency. *Circulation*. 2004;110:46–50.
- Yang Z, Day YJ, Toufektsian MC, Xu Y, Ramos SI, Marshall MA, French BA, Linden J. Myocardial infarct-sparing effect of adenosine A2A receptor activation is due to its action on CD4+ T lymphocytes. *Circulation*. 2006;114:2056–2064.
- Maisel A, Cesario D, Baird S, Rehman J, Haghighi P, Carter S. Experimental autoimmune myocarditis produced by adoptive transfer of splenocytes after myocardial infarction. *Circ Res*. 1998;82:458–463.
- Marty RR, Eriksson U. Dendritic cells and autoimmune heart failure. *Int J Cardiol*. 2006;112:34–39.

CLINICAL PERSPECTIVE

Cardiac remodeling after myocardial infarction is a major substrate for the development of heart failure. A significant component of this remodeling is orchestrated by the inflammatory response of the host. Innate immunity is the first-line defense mechanism of the host against external injury, triggering pathways involved in Toll/interleukin-1 receptor signaling. We found that interleukin-1 receptor-associated kinase (IRAK-4), a major regulator of innate immune response, has a surprising but essential role in modulating the post-myocardial infarction remodeling process through the functional regulation of dendritic cells. Targeted removal of IRAK-4 led to major benefits in survival and cardiac remodeling after infarction. This was accompanied by decreased bone marrow dendritic cell mobilization and impaired maturation. However, transfer of adult mature dendritic cells, after infarction was completed, annulled this protective benefit. Thus, the Toll/IRAK-4-dendritic cell axis has a detrimental effect on cardiac remodeling and may constitute a hitherto unrecognized new therapeutic target after infarction.

SUPPLEMENTAL MATERIAL

Supplemental Methods

Creation of MI

The mice were anesthetized with an intraperitoneal injection (IP) of ketamine (80mg/g) and xylazine (10mg/g), intubated and ventilated with a volume-cycled small-animal respirator. The heart was exposed through a left thoracotomy and MI was induced by ligating the left coronary artery with a prolene 6-0 suture. The mice that died within 24 hrs after the operation were excluded from the analysis. The sham-operated animals underwent the same procedure without ligation of the coronary artery.

Hemodynamics

Twenty-eight days after MI, the left ventricular performance was measured in mice anesthetized with isoflurane/oxygen (1.0%/100%). The animals were placed on controlled heating pads and core temperature measured via a rectal probe was maintained at $37 \pm 0.5^{\circ}\text{C}$. A microtip catheter transducer (SPR-839; Millar Instruments) was inserted into the right carotid artery and advanced into the left ventricle under pressure control. After stabilization for 15 min, the pressure signal was recorded continuously with an ARIA pressure-volume conductance system (Millar Instruments) coupled with a Powerlab/4SP A/D converter (AD Instruments).

Echocardiography

Transthoracic 2D, M-mode, and Doppler echocardiographic studies were performed with an Acuson Sequoia C256 system equipped with a 15-MHz linear transducer (15L8) (Version 4.0, Acuson Corp) in mice anesthetized with isoflurane/oxygen (1.0%/100%). M-mode tracings were recorded through the anterior and posterior LV walls at the papillary muscle level to measure LV end-diastolic dimension (LVEDD) and LV end-systolic dimension (LVESD). LV fractional shortening (FS) was calculated according to the following formula: $LV\ FS = [(LVEDD - LVESD) / LVEDD] \times 100$.

Morphometric analysis

After the physiological analysis, all surviving mice were euthanized and their hearts excised. The LVs were cut from apex to base into 3 transverse sections and were embedded in OCT compound (Sakura Finetechnical Co.), frozen in cold methanol, and cut by a cryostat into sections 5 μ m thick. Sections were stained with hematoxylin and eosin, Masson's trichrome, and picosirius red to determine the infarct size and collagen volume fraction and identify the gross morphology. The percentage of infarcted LV was estimated on day 28 by using planimetric techniques. Quantitative assessments of fibrotic area were performed on 20 randomly chosen high-power fields (X200) in each section by phase microscopy (Nikon) using the software of SimplePCI version 6 (Complex Inc. Image Systems).

DCs isolation from BM and in vitro activation of BMDCs

Dendritic cells (DCs) were isolated from bone marrow (BM) cells of WT and IRAK-4^{-/-} mice using a modified protocol described previously.¹ BM cells were cultured in RPMI 1640 medium (GIBCO) supplemented with penicillin (100U/ml, Sigma-Aldrich), streptomycin (100µg/ml, Sigma-Aldrich), 2-mercaptoethanol (50µM, Sigma-Aldrich), 10% FCS, 2.5 U/ml interleukin-4 (PeproTech Inc.) and 200 U/ml recombinant granulocyte-macrophage colony-stimulating factor (GM-CSF) (PeproTech Inc.) and medium was changed on days 3 and 6. On day 7, the non-adherent cells were collected, washed and resuspended in fresh medium with GM-CSF. The cells were plated at 1 X10⁶ cells/ml in 6-well plates for treatment with recombinant mouse heat shock protein (HSP) 70 (50 µg/ml) (Stressgen) or lipopolysaccharide (1µg/ml) (Sigma-Aldrich) for 24 hrs. Culture supernatants were removed after centrifugation and stored at -70°C.

Isolation of DCs from the heart

Heart-derived DCs were prepared as previously described.² To get DCs from whole heart cell suspensions, CD11c⁺ cells labeled by phycoerythrin (PE) were sorted using a FACSARIA flow cytometer (BD Biosciences). Isolated cardiac DCs were incubated on culture slides (BD Biosciences) with RPMI1640 and stained with Wright Giemsa (Sigma-Aldrich) to elucidate differences in the phenotypical characteristics between WT and IRAK-4^{-/-} mice after MI or sham operation.

Flow cytometry

Whole blood was drawn and subjected to red cell lysis using ACK lysing buffer (150 mM NH₄Cl, 10 mM KHCO₃, 10 mM EDTA), washed three times with buffer (PBS containing 1% FCS and 5 mM EDTA), and stained with antibodies for flow cytometric analyses to determine the percentage of DCs in peripheral blood. Single-cell suspensions from spleens were prepared to determine the percentage of DCs in the spleen as previously described.³ BMDCs and cardiac DCs were collected and stained for surface markers on ice after preincubation for 5 min with Fcγ III/II blocker (anti-CD16/CD32 antibody) (BD Pharmingen) to avoid nonspecific binding. Fluorescein isothiocyanate (FITC)-conjugated antibodies to mouse CD40, CD86, and major histocompatibility complex (MHC) class II and PE-conjugated to mouse CD11c and CD11b were purchased from BD Pharmingen and FITC-conjugated CD11c and CD80 was purchased from eBioscience. Cells were stained at 4°C in buffer, washed and resuspended in buffer containing 7-amino-actinomycin D to exclude dead cells. Samples were analyzed immediately using FACSCalibur and CellQuest software (BD Biosciences) or Cytomics FC500 and CXP software (Beckman Coulter). For each Ab, an isotype control of appropriate subclass (BD Pharmingen or eBioscience) was used.

Generation of necrotic cells

To obtain necrotic cells, freeze-thaw lysis was carried out on mouse embryonic fibroblasts

(MEFs) or HL-1 (cardiomyocyte cell line); the cells were exposed to five cycles of freezing on liquid nitrogen followed by thawing at 37°C. Such treatment generally resulted in lysis of 90% of the cells as judged by trypan blue inclusion. The supernatant of necrotic cells were added to DC suspensions for 24 hrs. All experiments were carried out under sterile conditions.

Western blotting

Frozen tissue was homogenized in lysis buffer (0.5% Triton X, 300 mM NaCl, 5 mM EDTA, 50 mM Tris (pH 7.6)) with protease inhibitor cocktail (Roche Applied Science). After centrifugation, 40 µg total protein per lane, estimated by the Bradford method with the use of a protein assay (Bio-Rad), was electrophoresed on a 4% to 12% gradient NuPAGE Bis-Tris gel (Invitrogen), and then electrophoretically transferred to polyvinylidene difluoride membranes. After blocking with 5% powdered skim milk in Tris-buffered saline (TBS) containing 0.1% Tween-20 at room temperature (RT) for 1 hr, the membrane was incubated with the primary antibody; anti-IRAK-4 antibody (Upstate Biotechnology Inc), anti-I-kappa-B (IκB)α antibody, anti-phospho-IκBα antibody, anti-I-kappa-B kinase (IKK)α antibody, anti-IKKβ antibody, anti-phospho-IKKα/β antibody, anti-nuclear factor κB (NF-κB) p65 antibody, anti-phospho-NF-κB p65 antibody (Cell signaling), anti-inducible nitric oxide synthase antibody (BD Bioscience) and anti-glyceraldehyde 3-phosphate dehydrogenase antibody (Santa Cruz) at 4°C overnight or for 1 hr at RT, and then incubated with secondary horseradish peroxidase (HRP)

conjugated antibody for 1 hr at RT. Chemiluminescence was detected with an ECL Western blot detection kit (Amersham Pharmacia) according to the manufacturer's recommendation. The bands on the x-ray film were scanned with GS-800 (Bio-Rad) and analyzed using the Quantity One software (Bio-Rad).

Immunohistochemistry

Cryostat sections (7µm) were cut from hearts, air-dried, and fixed in acetone at RT for 10 min or in 4% paraformaldehyde at RT for 20 min. Endogenous peroxidase activity was blocked with 0.3% hydrogen peroxide (Sigma-Aldrich) in PBS for 20 min. Reaction with primary anti-CD45, anti-Mac-3, anti-CD11c (BD Pharmingen), and anti-neutrophil and anti-CD3 (Serotec) antibodies were performed 1 hr at RT or overnight at 4°C. Following incubation with the primary antibodies, the Vectastain ABC elite Kit (Vector Labs) was used according to the manufacturer's instructions or anti-rat HRP IgG antibody was used as the secondary antibody before visualization with 3,3'-diaminobenzidine. The sections were finally counterstained with hematoxylin. As negative controls, the same procedures were performed but without the primary antibodies. For the assessment of CD3⁺ T-lymphocytes activation, sections were stained with an anti-CD3 and an anti-CD154 (BD Pharmingen) primary antibody followed by the addition of a FITC-conjugated and a TRITC-conjugated secondary antibody. Nuclei were identified with DAPI.

Analysis of myocardial apoptosis

To detect apoptosis, LV tissue sections were stained with terminal deoxynucleotidyl transferase-mediated dUTP nick end-labeling (TUNEL) staining (Chemicon). Anti- α -actinin (Sigma-Aldrich) was used to identify cardiomyocytes. The number of TUNEL-positive nuclei was counted, and the data were normalized per total nuclei identified by DAPI-staining (Invitrogen) in the same sections. We also examined cleaved and uncleaved caspase-3 levels in the infarcted myocardium by immunoblotting. Caspase-3 antibody (Cell Signaling) was used in the immunoblotting. Proteins were visualized with an enhanced chemiluminescence detection system.

Preparation of nuclear protein extracts

Heart tissue was rinsed with ice-cold PBS and homogenized on ice in 1 ml of ice-cold Buffer I (10 mM HEPES (pH 8.0), 1.5 mM MgCl₂, 10 mM KCl, 1 mM DTT, protease inhibitor cocktail). After 15 min incubation on ice to allow cells to swell, 1% NP-40 was added and homogenates were centrifuged at 15000 rpm for 3 min at 4°C. The supernatants were discarded, and the pellets were suspended in ice-cold Buffer II (20 mM HEPES (pH 8.0), 25% glycerol, 420 mM NaCl, 1.5 mM MgCl₂, 0.2 mM EDTA, 1 mM DTT, protease inhibitor cocktail) incubated at 4°C for 30 min, and then centrifuged. The supernatants were transferred in aliquots to new tubes and stored at -70°C until analyzed.

Electrophoretic Mobility Shift Assay (EMSA)

Activation of NF- κ B was evaluated by electrophoretic mobility shift assay (EMSA) according to the manufacturer's instructions (The LightShift® Chemiluminescent EMSA Kit, Pierce). Biotin end-labeled DNA duplex of sequence 5'-AGT TGA GGG GAC TTT CCC AGG C-3' and 3'-TCA ACT CCC CTG AAA GGGTCC G-5' containing a putative binding site for NF- κ B was incubated with the nuclear extracts. After the reaction the DNA-protein complexes were subjected to a 6% native polyacrylamide gel electrophoresis and transferred to a nylon membrane (Bio-Rad). After transfer the membrane was immediately cross-linked for 1 min on a UV transilluminator equipped with 254 nm bulbs. A chemiluminescent detection method utilizing a luminol/enhancer solution and a stable peroxide solution (Pierce) was used as described by the manufacturer protocol, and membranes were exposed to x-ray films before developing. The bands were scanned with GS-800 (Bio-Rad) and analyzed using the Quantity One software (Bio-Rad).

TNF- α , IL-6, and IL-12p70 measurements

TNF- α , IL-6, and IL-12p70 concentration in culture supernatants were measured by Bio-Plex mouse cytokine assays (Bio-Rad).

Allogeneic Mixed Lymphocyte Reaction (MLR)

The capacity of BMDCs from WT or IRAK-4^{-/-} mice on T cell activation was evaluated in a

primary allogeneic MLR. Non-irradiated DCs were harvested after 24 hrs of maturation with TNF- α (50ng/ml) and used as T cell stimulators. B-cell depleted Balb/c splenocytes by BioMag[®] anti-mouse IgG-magnetic beads (QIAGEN) were used as responder cells. The splenocytes were labeled with the fluorescent dye 5, 6-carboxyfluorescein diacetate succinimidyl ester (CFSE) (Molecular Probes). With each cell division, the fluorescence intensity of the cells is reduced by half. Culture medium consisted of RPMI 1640 supplemented with 10% FCS, 2-mercaptoethanol (50 μ M), N-acetyl cysteine (3.3 mM), penicillin (100 U/ml) and streptomycin (100 μ g/ml). CFSE-labeled splenocytes were plated at 1×10^6 cells/ml in a volume of 100 μ l per well in duplicates and co-cultured with 100 μ l of 1.25×10^5 cells/ml of DCs at a final ratio of 8:1 (responder:stimulator) in 96-well U-bottom plates. After 6 days of co-culture in 5% CO₂ at 37°C, cells were harvested, washed with PBS and stained with mouse anti-mouse CD4-PE (BD Pharmingen) and 7-AAD. Three-color flow cytometry was performed to trace the CFSE-decline in CD4⁺ cells.

Quantification of gene expression by real-time Polymerase Chain Reaction (PCR)

Total RNA was extracted from infarcted myocardium and 10^{4-5} cardiac DCs and T-lymphocytes samples using Trizol Reagent (Invitrogen) according to the manufacturer's protocol. Reverse transcription was performed with aliquots of each RNA sample, random hexamers, and superscript reverse transcriptase according to the protocol of the Super-Script First-Strand

Synthesis System for RT-PCR (Invitrogen). Real-time quantitative PCR was performed using an ABI Prism 7000 sequence detector (PE Applied Biosystems) or LightCycler 480 Instrument. The sequences of primer pairs specific for mouse IL-1 β , IL-6, TNF- α , IL-12a, IL-12b, CD80, CD86, CCL2 (chemokine (C-C motif) ligand 2), CCL5 (chemokine (C-C motif) ligand 5), MIP(macrophage inflammatory protein)-1 α , MIP-1 β , and 18S were designed using the Primer Express II software (PE Applied Biosystems) or Vector NTI suite 9 (Invitrogen); see supplemental Table 1 for details. PCR reactions were performed according to the manufacturer's instructions. Cytokine mRNA levels are presented as the mean \pm SEM fold increase in gene expression observed in duplicate wells of target samples relative to control samples. The obtained CT (cycle number at which an amplification threshold of detection is reached) values were normalized to murine 18S rRNA expression by the $\Delta\Delta$ Ct method using trough sham levels as the calibrator value.⁴

Migration assay

Cell migration was evaluated using a 48-well chemotaxis chamber (Neuroprobe) and polycarbonate filters (5- μ m pore size; Neuroprobe) as previously described.⁵ Cell suspensions (1X10⁶/ml) were incubated at 37°C for 90 min. Results are expressed as number of migrated cells in an average of 4 high-power fields (100X). Mouse recombinant MIP -1 α , MIP-1 β , CCL2 and CCL5 (Peprotech Inc.) were used as chemoattractant agonists.

Cytokine Treatment Protocol

Mice were injected once daily with 100ng recombinant mouse GM-CSF (PeproTech Inc.) and stromal cell-derived factor-1 (SDF-1) (Millipore) for 7 consecutive days intravenously. PBS was used in control injections. The presence of circulating recombinant mouse GM-CSF and SDF-1 was determined on day 7 serum samples by specific enzyme-linked immunosorbent assay (R&D system).

Supplemental Table 1 Primers for real-time PCR

Gene	Sequence
IL-1 β	(F)TTGGGCCTCAAAGGAAAGAAT (R)TGGGTATTGCTTGGGATCCA
IL-6	(F)GCTAAGGACCAAGACCATCCAAT (R)GGCATAACGCACTAGGTTTGC
TNF- α	(F)GCCAACGGCATGGATCTC (R)GCAGCCTTGTCCTTGAAGAG
IL-12a	(F)GACCCTGTGCCTTGGTAGCA (R)TGCTGATGGTTGTGATTCTGAAG
IL-12b	(F)GCCAGTACACCTGCCACAAA (R)TTAAAATTTTCAGTGGACCAAATTCC
CD80	(F)TTGTGCTGCTGATTCGTCTTTC (R)TGTAACGGCAAGGCAGCAA
CD86	(F)TTCATTCCCGGATGGTGTGT (R)TCTTGAGTGAAATTGAGAGGTTTGG
CCL2	(F)GCTGGAGCATCCACGTGT (R)CTGCTGCTGGTGATCCTCTT
CCL5	(F)TGCTTTGCCTACCTCTCCC (R)CAAACACGACTGCAAGATTGG
MIP-1 α	(F)GCA ACC AAG TCT TCT CAG CGC (R)ACA CCT GGC TGG GAG CAA AG
MIP-1 β	(F)TGCTCGTGGCTGCCTTCT (R)TGAAGCTGCCG GGAGGTGTA
18S	(F)TCGGA ACTGAGGCCATGATT (R)CCTCCGACTTTCGTTCTTGATT

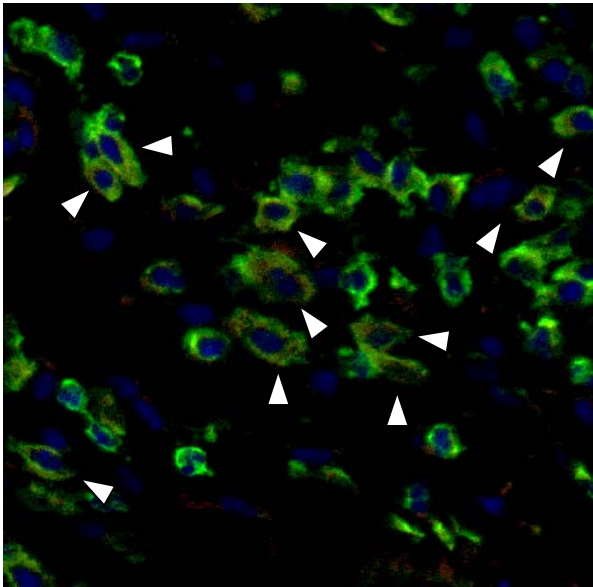
(F), Forward Primer; (R), Reverse Primer.

References

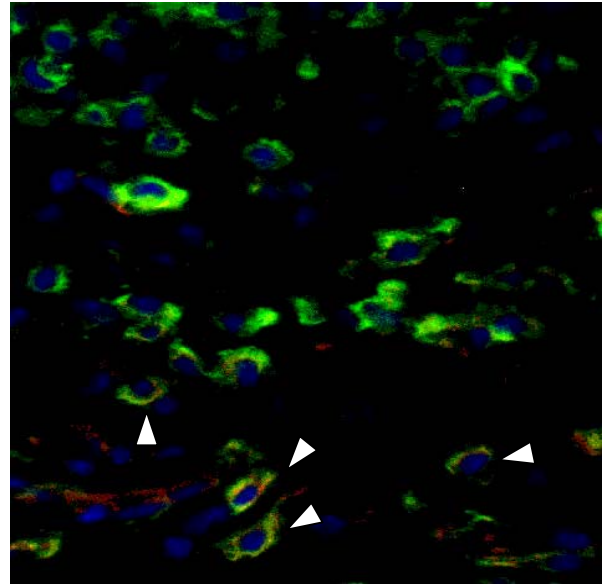
1. Lutz MB, Kukutsch N, Ogilvie AL, Rossner S, Koch F, Romani N, Schuler G. An advanced culture method for generating large quantities of highly pure dendritic cells from mouse bone marrow. *J Immunol Methods*. 1999;223:77-92.
2. Austyn JM, Hankins DF, Larsen CP, Morris PJ, Rao AS, Roake JA. Isolation and characterization of dendritic cells from mouse heart and kidney. *J Immunol*. 1994;152:2401-10.
3. Inaba K, Swiggard WJ, Steinman RM, Romani N, Schuler G. Isolation of dendritic cells. *Curr Protoc Immunol*. 2001;Chapter 3:Unit 3 7.
4. Maekawa Y, Anzai T, Yoshikawa T, Sugano Y, Mahara K, Kohno T, Takahashi T, Ogawa S. Effect of granulocyte-macrophage colony-stimulating factor inducer on left ventricular remodeling after acute myocardial infarction. *J Am Coll Cardiol*. 2004;44:1510-20.
5. Sozzani S, Sallusto F, Luini W, Zhou D, Piemonti L, Allavena P, Van Damme J, Valitutti S, Lanzavecchia A, Mantovani A. Migration of dendritic cells in response to formyl peptides, C5a, and a distinct set of chemokines. *J Immunol*. 1995;155:3292-5.

The online data supplement Figure 1A.

WT

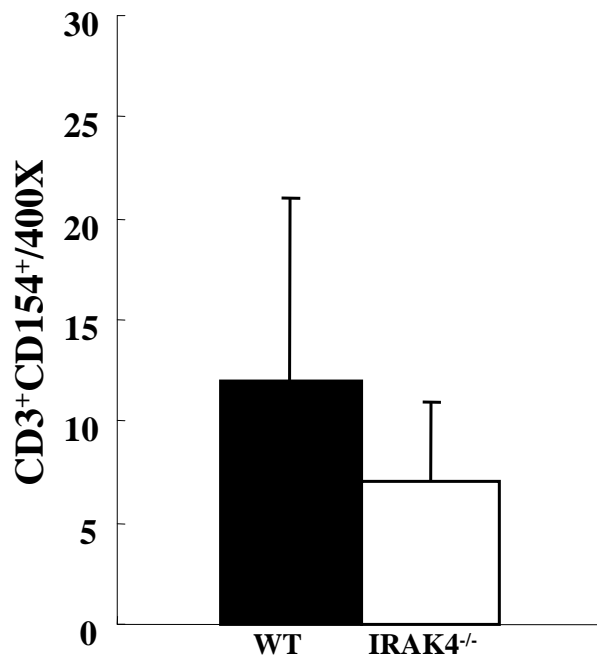


IRAK-4^{-/-}



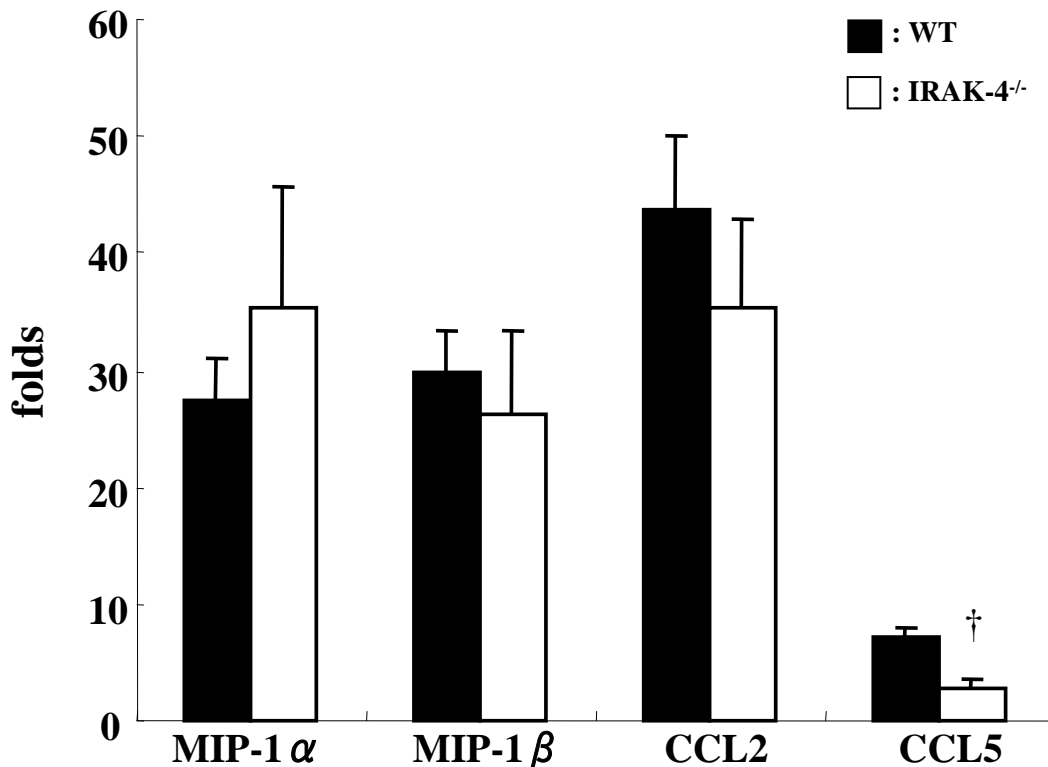
The online data supplement Figure 1A. Infiltration of activated CD3⁺ T-lymphocytes into injured myocardium of WT and IRAK-4^{-/-} mice after MI. Activated CD3⁺ T-lymphocytes are yellowish because of overlap of CD3 (green) and CD154 (red) staining. Magnification, x400.

The online data supplement Figure 1B.



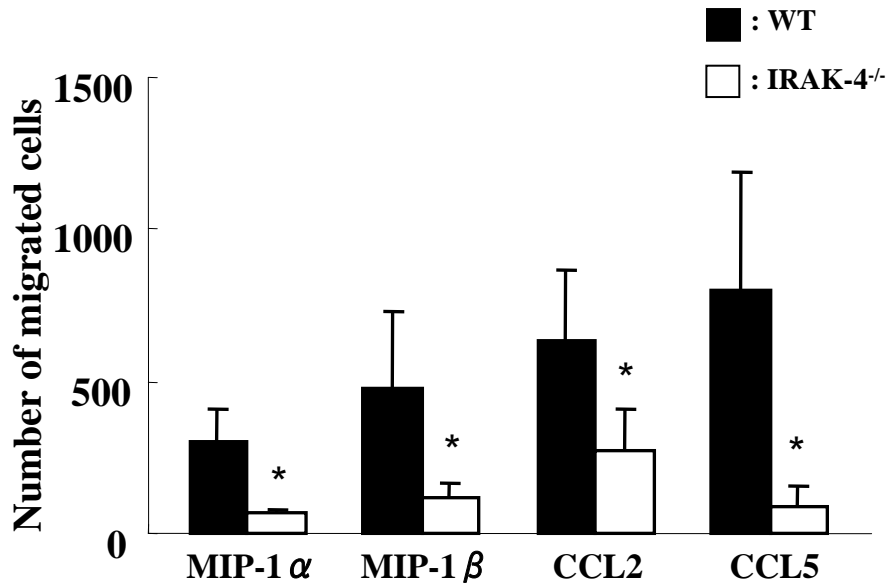
The online data supplement Figure 1B. Quantification of activated CD3⁺ T-lymphocytes into injured myocardium of WT and IRAK-4^{-/-} mice after MI.

The online data supplement Figure 2.



The online data supplement Figure 2. Chemokines expression in the infarcted heart of WT and IRAK-4^{-/-} mice. MIP-1 α , MIP-1 β , CCL2 and CCL5 expression of infarcted myocardium of MI-operated WT (black bar) and IRAK-4^{-/-} mice (white bar) on Day 3 (n= 3 to 6). [†]P<0.05 vs. WT MI.

The online data supplement Figure 3.



The online data supplement Figure 3. Migration ability of BMDCs from WT and IRAK-4^{-/-} mice. Migration of BMDCs from WT (black bar) and IRAK-4^{-/-} mice (white bar) in response to 100ng/ml of MIP-1 α , MIP-1 β , CCL2 and CCL5. Data are the mean \pm SEM of cells from 4 individual fields from a representative experiment of 3 repetitions. *P<0.05 vs. WT.